HEP 2019 - Conference on Recent Developments in High Energy Physics and Cosmology 17-20 April 2019, NCSR "DEMOKRITOS", Athens, Greece

Recent Developments on Precision Timing with PICOSEC-Micromegas Detectors

Performance, Modeling and Applications

Spyros Eust. Tzamarias
Aristotle University of Thessaloniki
on behalf of the
RD51 PICOSEC-Micromegas Collaboration

ARISTOTLE UNIVERSITY OF THESSALONIKI

PICOSEC Micromegas

Timing with a few 10's of picosecond

- Needs for Precise timing bring us to the picosec domain
- E.g., in the High Luminosity LHC, 140-200 "pile-up" proton-proton interactions ("vertices") with happen in the same LHC clock, in close space (Gaussian +- 45mm).
- Using precise timing can separate particles coming from the various vertices.
- (3D) tracking of charged particles is not enough to associate them to the correct vertex . Including precise time offers an extra dimension of separation to achieve this.
- Needed precision
- ~ order 30ps

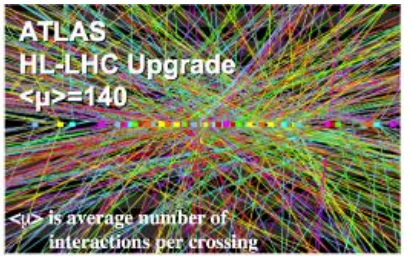

The association of the time measurement to the energy measurement is crucial for physics analysis, and requires time resolution of 20-30ps.

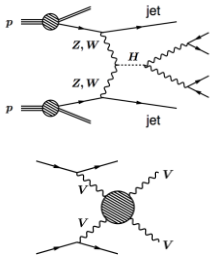

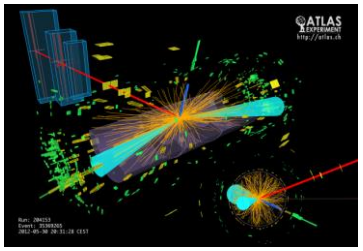

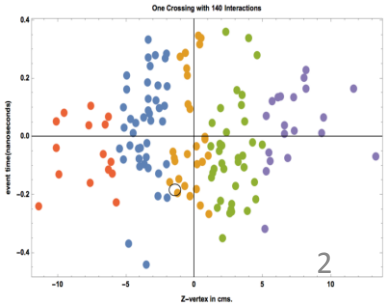

Existing Instrumentation:

e.g. Multi-Channel Plate (MCP) with σ_t~ 4ps but very expensive for large area coverage

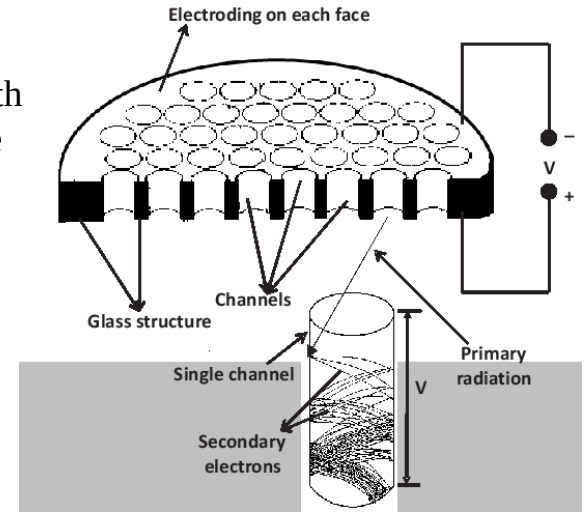

PhotoMultiplier: σ_t >800ps

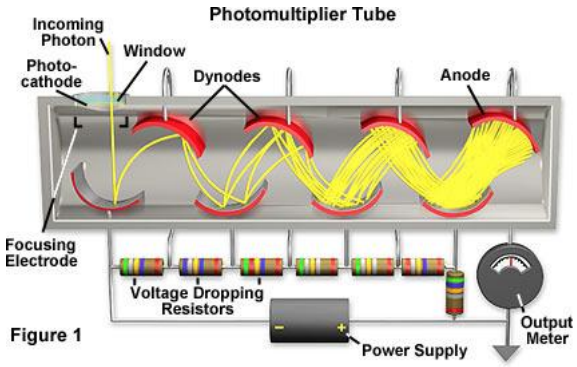

Figure 1

Since the hermetic approach at the LHC experiments requires large area coverage, it is natural to investigate both MicroPattern Gas and Silicon structures as candidate detector technologies. However, since the necessary time resolution for pileup mitigation is of the order of 20-30 ps, both technologies require significant modification to reach the desired performance.

Large area detectors, resistant to radiation damage, with ~10ps timing capabilities will find applications in many other domains, e.g.

- particle identification in Nuclear and Particle Physics experiments
- photon's energy/speed measurements and correlations for Cosmology
- optical tracking for charge particles
- 4D tracking in the future accelerators (e.g. FCC with a center energy of ~100TeV)

MicroMegas: Micro Pattern Gaseous Chambers

Nuclear Instruments and Methods in Physics Research A 376 (1996) 29–35

NUCLEAR INSTRUMENTS & METHODS IN PHYSICS RESEARCH Section A

MICROMEGAS: a high-granularity position-sensitive gaseous detector for high particle-flux environments

Y. Giomataris[a,*], Ph. Rebourgeard[a], J.P. Robert[a], G. Charpak[b]

[a]CEA/DSM/DAPNIA/SED-C.E.-Saclay, 91191 Gif/Yvette, France
[b]Ecole Superieure de Physique et Chimie Industrielle de la ville de Paris, ESPECI, Paris, ESPCI, Paris, France and CERN/AT, Geneva, Switzerland

Received 24 January 1996

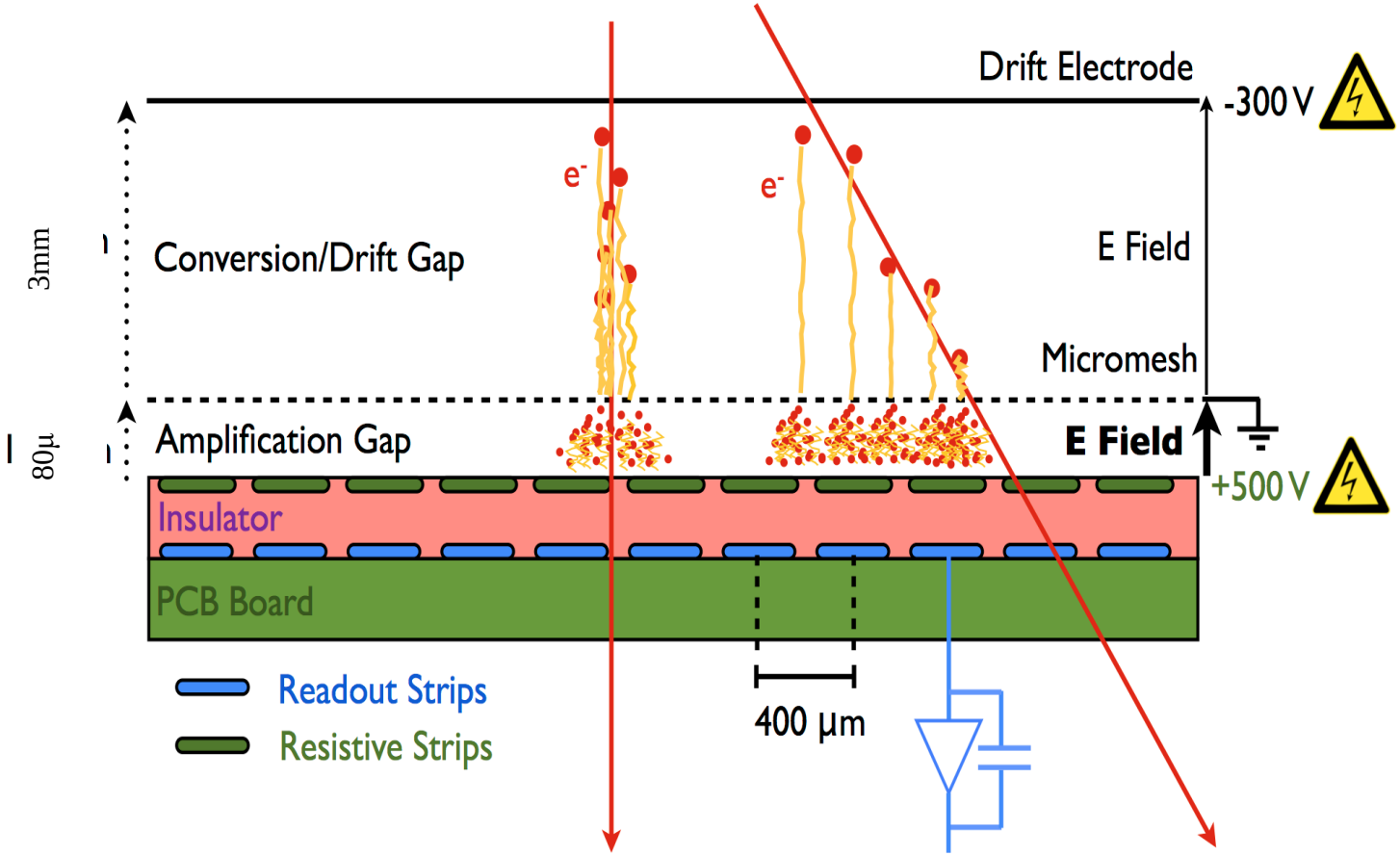

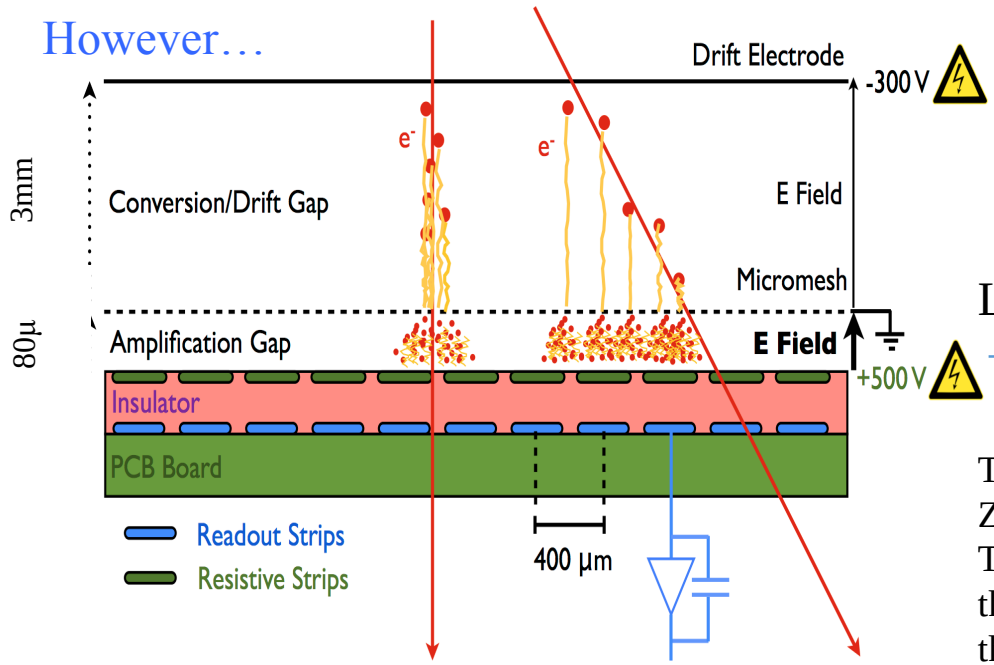

Using the drift velocity (V), we express the probability that the first electrons will reach the anode at time t as:

$$A^n_{first}(t) = n(V/L)e^{-nVt/L}$$

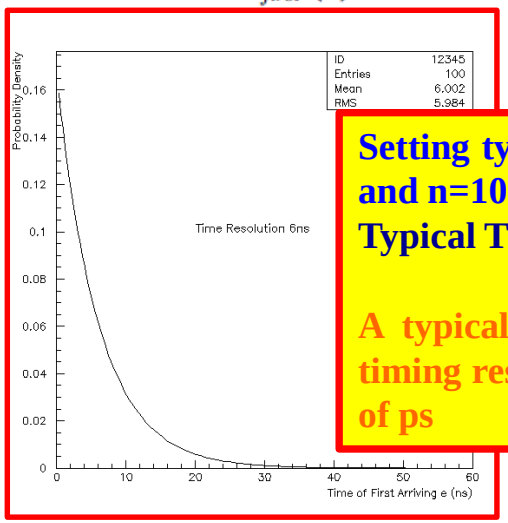

Setting typical values, i.e. V=50µm/ns and n=10 we conclude that:
Typical Time Resolution ~6ns

A typical MicroMegas cannot reach timing resolution at the level of tenths of ps

Let n be the mean number of the e-ion pairs produced by the charged particle along its track. Then the probability that k-pairs are produced by a single track is given by the Poisonian

$$P^n_k = \frac{n^k}{k!} e^{-n}$$

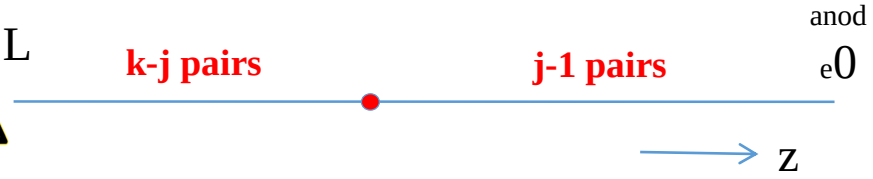

The probability that an e-ion pair has been produced at Z=z is the same for any value of Z; **p=1/L**
Then, in case that k pairs are produced, the probability that the jth pair has been produced at Z= z is given by the binomial distribution

$$D^k_j(x) = \frac{k!}{(k-j)!(j-1)!}(1-x)^{k-j}x^{j-1}$$

where **x=z/L describes the probability that a pair is produced in the region 0-z**

The probability that the jth pair has been produced at Z= z for any total number of e-ion pairs is given by

$$A^n_j(x) = \sum_{k=j}^{\infty} P^n_k D^k_j(x) = \frac{x^{j-1}}{(j-1)!} n^j e^{-nx}$$

The probability that the last pair (i.e. the closest to the edge 0) has been produced at Z= z is given by (j-1=0):

$$A^n_{last}(x) = ne^{-nx}$$
$$A^n_{last}(z) = ne^{-nz/L}$$

The Physics of Ionization offers the means for precise spatial measurements (high spatial resolution) but inhibits precise timing measurements

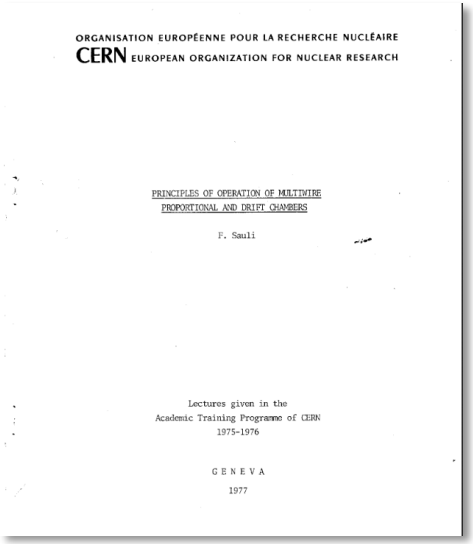

ORGANISATION EUROPÉENNE POUR LA RECHERCHE NUCLÉAIRE
CERN EUROPEAN ORGANIZATION FOR NUCLEAR RESEARCH

PRINCIPLES OF OPERATION OF MULTIWIRE PROPORTIONAL AND DRIFT CHAMBERS

F. Sauli

Lectures given in the
Academic Training Programme of CERN
1975-1976

GENEVA
1977

which is represented in Fig. 8, for n = 34, as a function of the coordinate across a 10 mm thick detector. If the time of detection is the time of arrival of the closest electron at one end of the gap, as is often the case, the statistics of ion-pair production set an obvious limit to the time resolution of the detector. A scale of time is also given in the figure, for a collection velocity of 5 cm/μsec typical of many gases; the FWHM of the distribution is about 5 nsec. There is no hope of improving this time resolution in a gas counter, unless some averaging over the time of arrival of all electrons is realized.

The ouroboros or uroborus from Greek οὐροβόρος from οὐρά, "tail," and -βορος, "devouring") is an ancient symbol depicting a serpent or dragon eating its own tail. Originating in ancient Egyptian iconography, the ouroboros entered western tradition via Greek magical tradition and was adopted as a symbol in Gnosticism and Hermeticism, and most notably in alchemy. Via medieval alchemical tradition, the symbol entered Renaissance magic and modern symbolism, often taken to symbolize introspection, the eternal return or cyclicality, especially in the sense of something constantly re-creating itself. **It also represents the infinite cycle of nature's endless creation and destruction, life and death.**

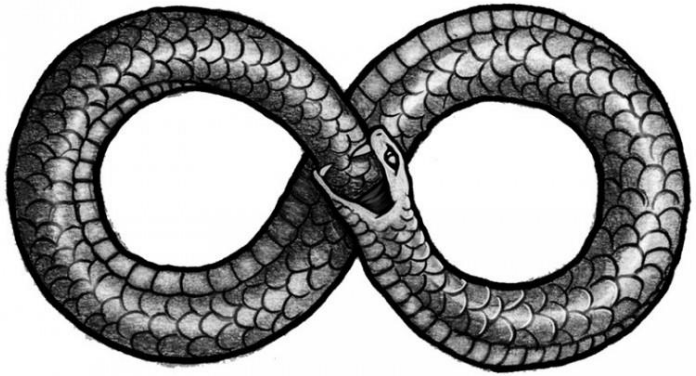

In order to use gaseous detectors for precise (ps) timing of charge particles we should turn other Physics phenomena against the stochastic Nature of ionization

MicroMegas PICOSEC detector concept

PICOSEC is a hybrid
a two-stage MicroMegas
with Cerenkov radiator
and
a photocathode layer

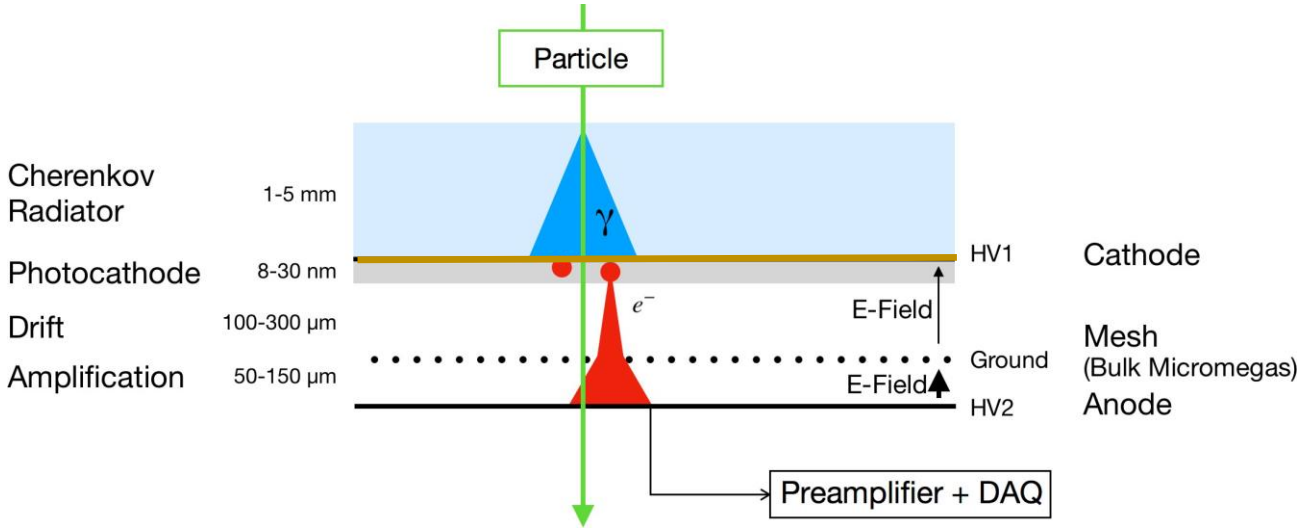

- Radiator: Particle passage produce Cherenkov UV light
- Photocathode: UV → photoelectrons, emitted ~ synchronously;
- These electrons enter the thin-gap MicroMegas chamber, in the “drift”/”pre-amplification” gap: which is small (~200microns) with high-field (~500V), and soon each electron initiates an avalanche in this region. Due to high gain in drift region jitter before first amplification minimised
- Via the mesh, a fraction of these pre-amplification avalanche electrons pass to the lower “amplification” region, where each one starts a new avalanche and induces signal on the anode.
- → depending on how big is the (circular of hexagonal) readout-pad on the anode, it can see full or partial signal from the Cerenkov cone

PICOSEC concept and specifics

Radiator: MgF_2 (3mm thick)
Photocathode:
CsI, metal, Diamond-Like Carbon

Drift gap = 200 μm
Amplification gap = 128 μm
Mesh thickness = 36 μm
(centered at 128 μm above anode)

COMPASS gas
(80% Ne + 10% CF_4 + 10% C_2H_6)
Pressure: 1 bar.

Anode voltage = 450 V
→ E = 35 kV/cm
Cathode voltage = 300-425 V
→ E in [15, 21] kV/cm

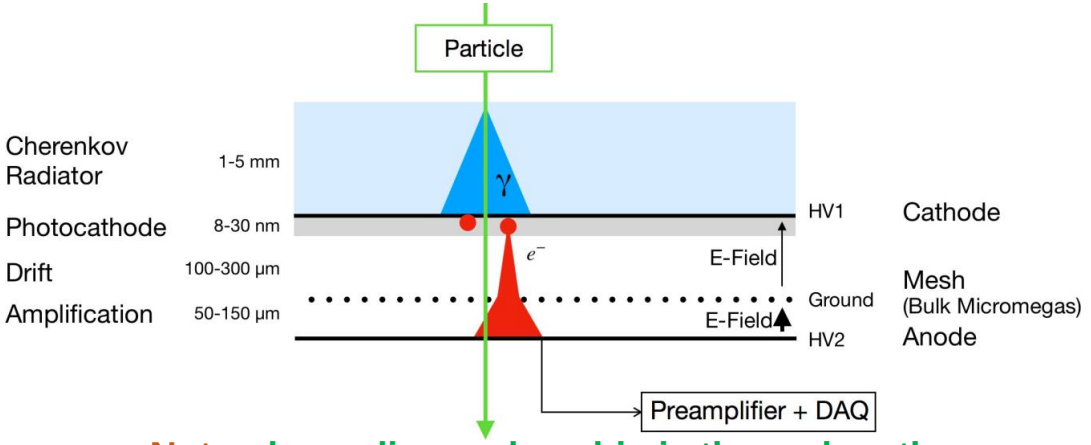

Note: depending on how big is the pad on the anode, it can see full or partial signal from the Cerenkov cone

Two-component signal:
*** Electron peak ("e-peak") → fast (~0.5ns)**
*** Ion tail (~100ns)**

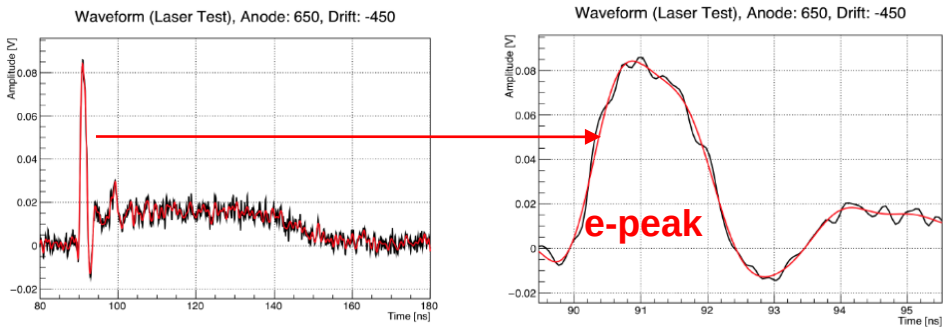

Signal from Laser runs (right is zoom in e-peak)

Digitized Waveforms (at 50-100 ps sampling)
Time signal arrival with Constant Fraction Discrimination at 20% of e-

Single-pad prototype

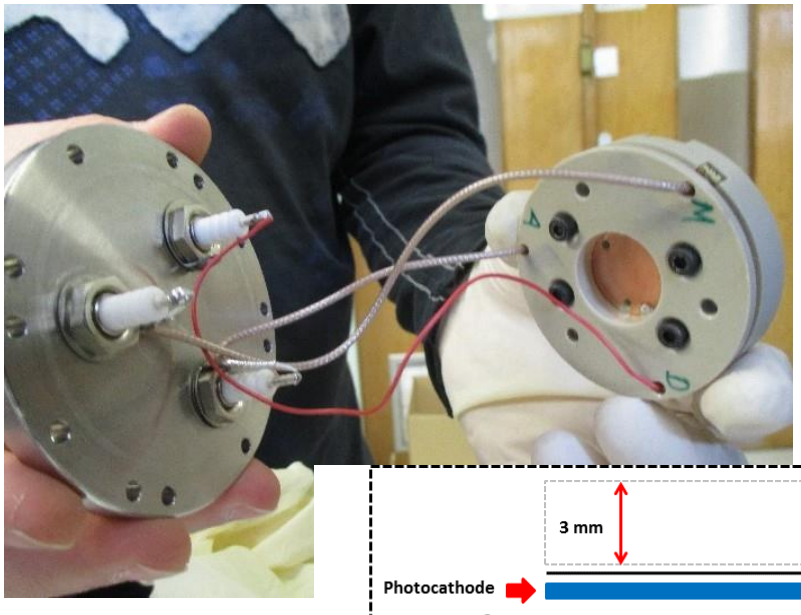

→ 1 large channel : 1cm diameter active area

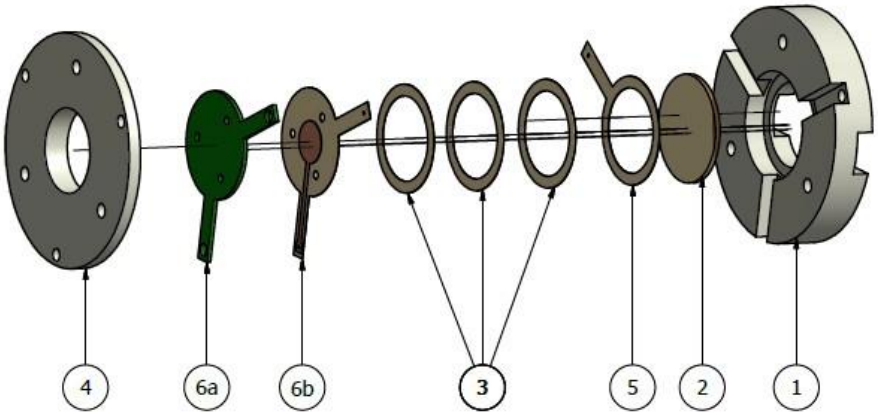

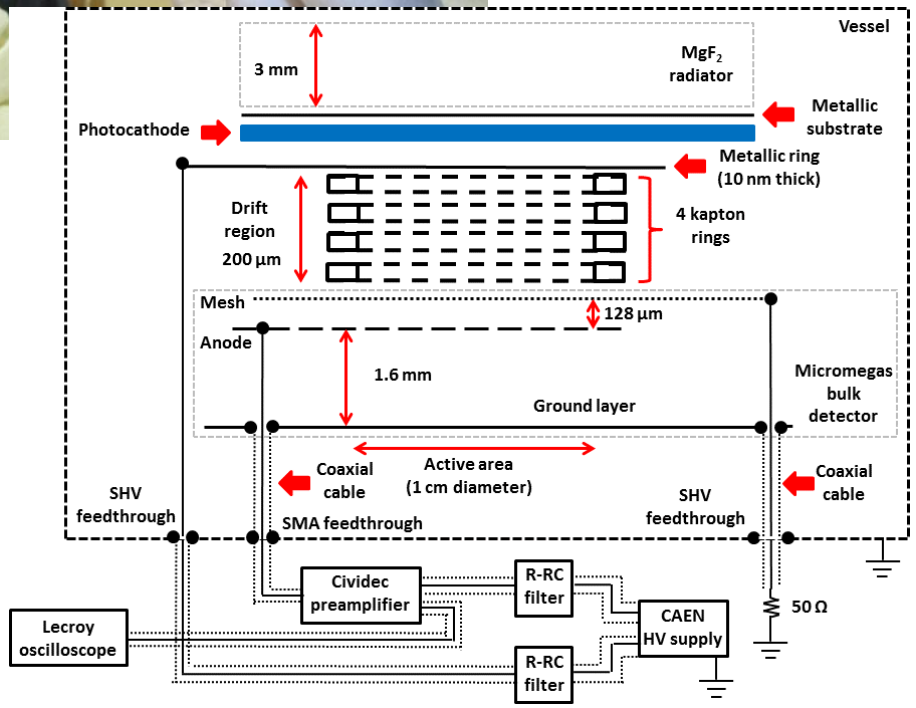

Testing prototypes in Particle and laser Beams

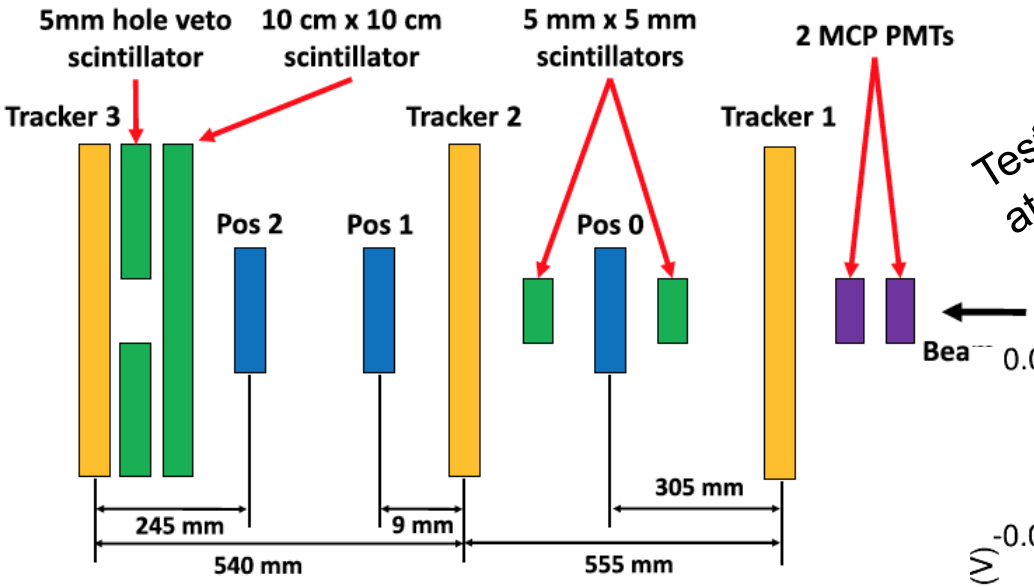

Testbeam at CERN

Muon beams & UV light
3 GEMs for tracking
and
* MCP for reference time (red): <4ps accurancy
* PICOSEC: blue

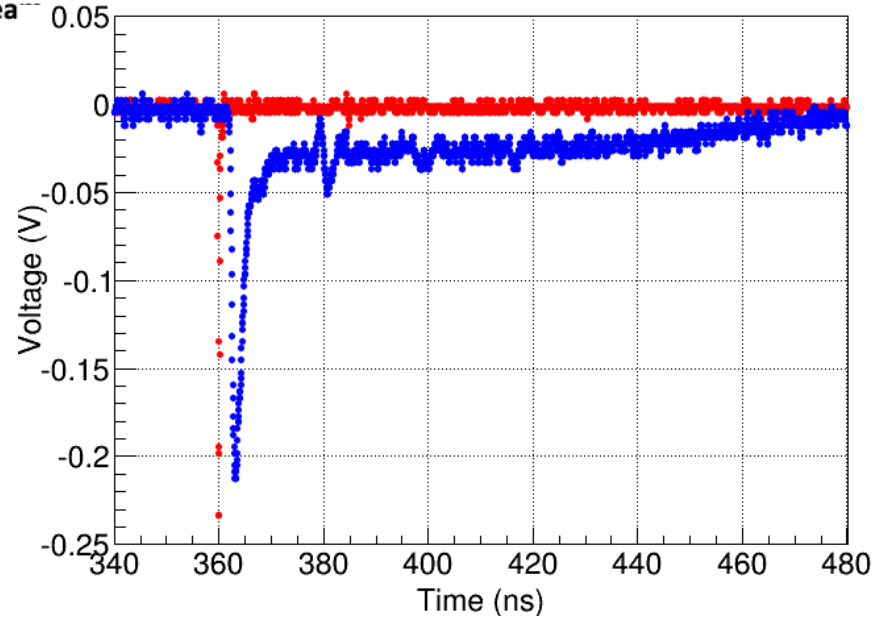

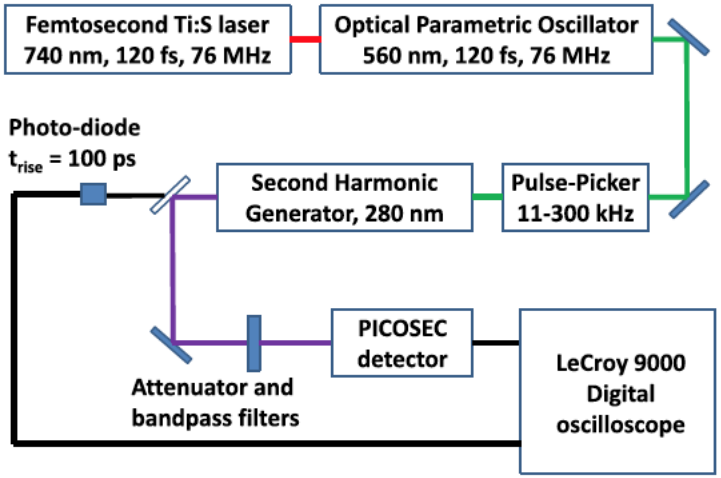

Laser at Saclay

Nuclear Inst. and Methods in Physics Research, A 903 (2018) 317–325

Contents lists available at ScienceDirect

Nuclear Inst. and Methods in Physics Research, A

journal homepage: www.elsevier.com/locate/nima

PICOSEC: Charged particle timing at sub-25 picosecond precision with a Micromegas based detector

J. Bortfeldt [b], F. Brunbauer [b], C. David [b], D. Desforge [a], G. Fanourakis [e], J. Franchi [b], M. Gallinaro [g], I. Giomataris [a], D. González-Díaz [i], T. Gustavsson [j], C. Guyot [a], F.J. Iguaz [a,*], M. Kebbiri [a], P. Legou [a], J. Liu [c], M. Lupberger [b], O. Maillard [a], I. Manthos [d], H. Müller [b], V. Niaouris [d], E. Oliveri [b], T. Papaevangelou [a], K. Paraschou [d], M. Pomorski [k], B. Qi [c], F. Resnati [b], L. Ropelewski [b], D. Sampsonidis [d], T. Schneider [b], P. Schwemling [a], L. Sohl [b,1], M. van Stenis [b], P. Thuiner [b], Y. Tsipolitis [f], S.E. Tzamarias [d], R. Veenhof [h,2], X. Wang [c], S. White [b,3], Z. Zhang [c], Y. Zhou [c]

[a] IRFU, CEA, Université Paris-Saclay, F-91191 Gif-sur-Yvette, France
[b] European Organisation for Nuclear Research (CERN), CH-1211 Geneva 23, Switzerland
[c] State Key Laboratory of Particle Detection and Electronics, University of Science and Technology of China, Hefei 230026, China
[d] Department of Physics, Aristotle University of Thessaloniki, Thessaloniki, Greece
[e] Institute of Nuclear and Particle Physics, NCSR Demokritos, 15341 Agia Paraskevi, Attiki, Greece
[f] National Technical University of Athens, Athens, Greece
[g] Laboratório de Instrumentação e Física Experimental de Partículas, Lisbon, Portugal
[h] RD51 collaboration, European Organization for Nuclear Research (CERN), CH-1211 Geneva 23, Switzerland
[i] Instituto Galego de Física de Altas Enerxías (IGFAE), Universidade de Santiago de Compostela, Spain
[j] LIDYL, CEA-Saclay, CNRS, Université Paris-Saclay, F-91191 Gif-sur-Yvette, France
[k] CEA-LIST, Diamond Sensors Laboratory, CEA Saclay, F-91191 Gif-sur-Yvette, France

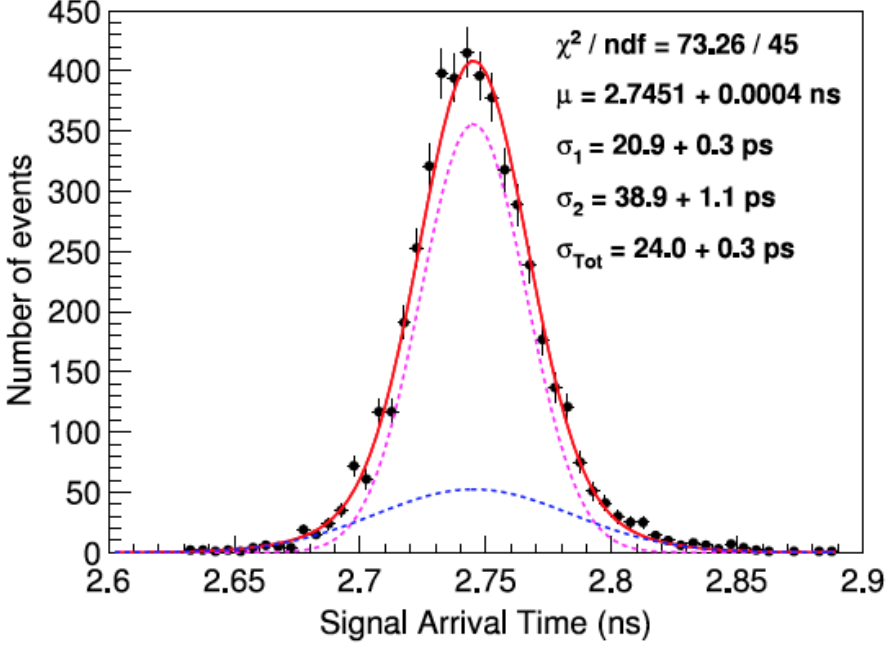

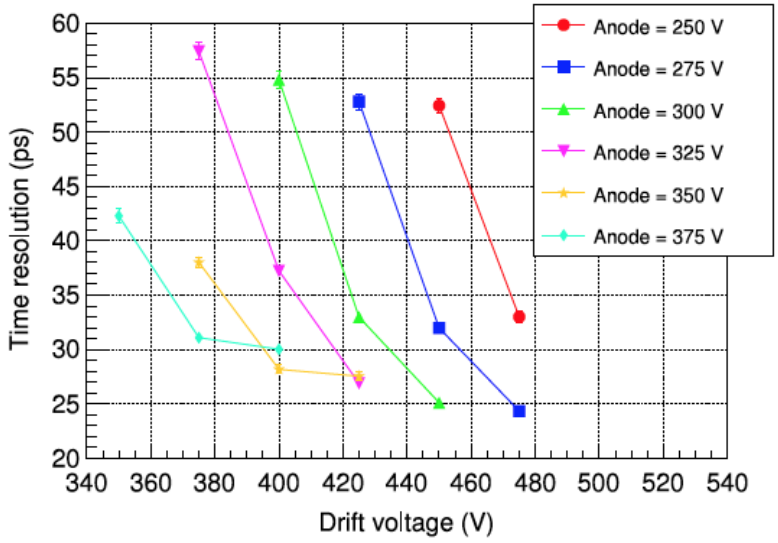

80 ps Timing Resolution for single-photon

Timing Resolution depends strongly on the drift voltage and less on the amplification field

The Signal Arrival Time (SAT) depends on the e-peak size in a non-trivial way

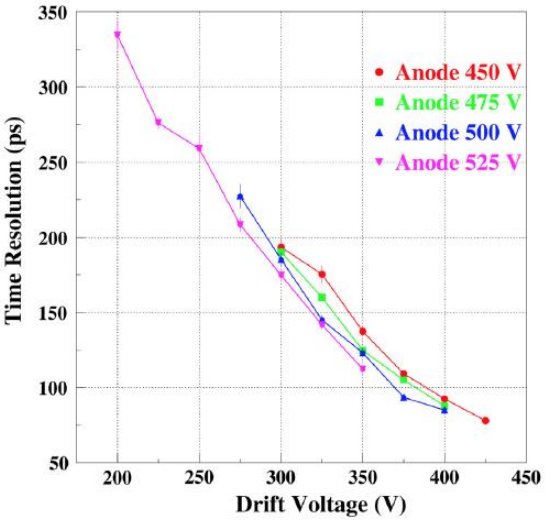

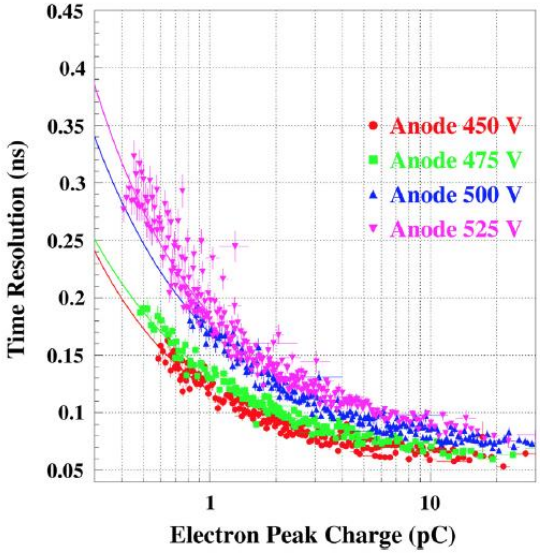

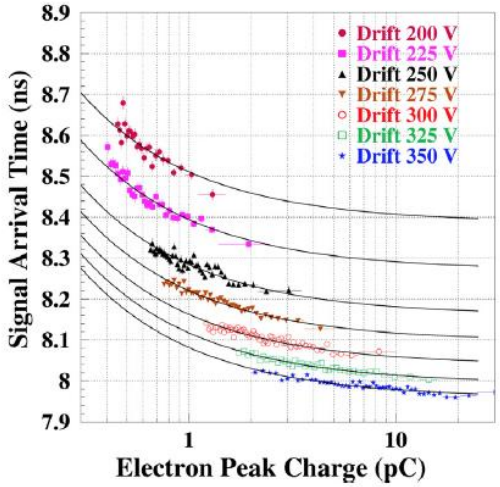

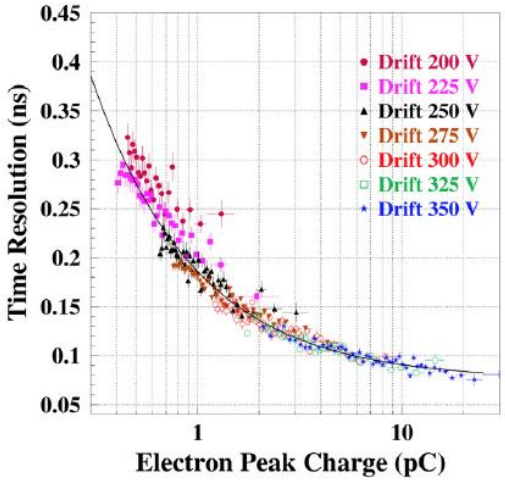

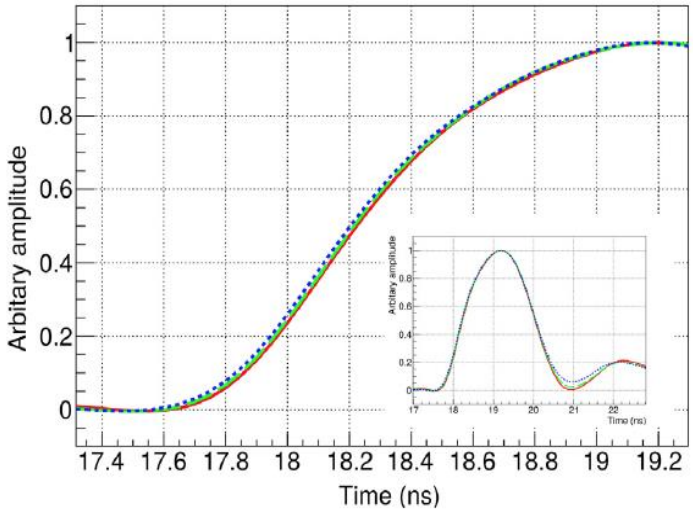

Identify the microscopic parameters which determine the Timing Characteristics

The details in the Garfield++ simulation (1)

Use Garfield++ to simulate PICOSEC for single photoelectrons

COMPASS gas
(80% Ne + 10% CF_4 + 10% C_2H_6)
Pressure: 1 bar.

ANSYS for the electric field

Drift gap = 200 μm
Amplification gap = 128 μm
Mesh thickness = 36 μm

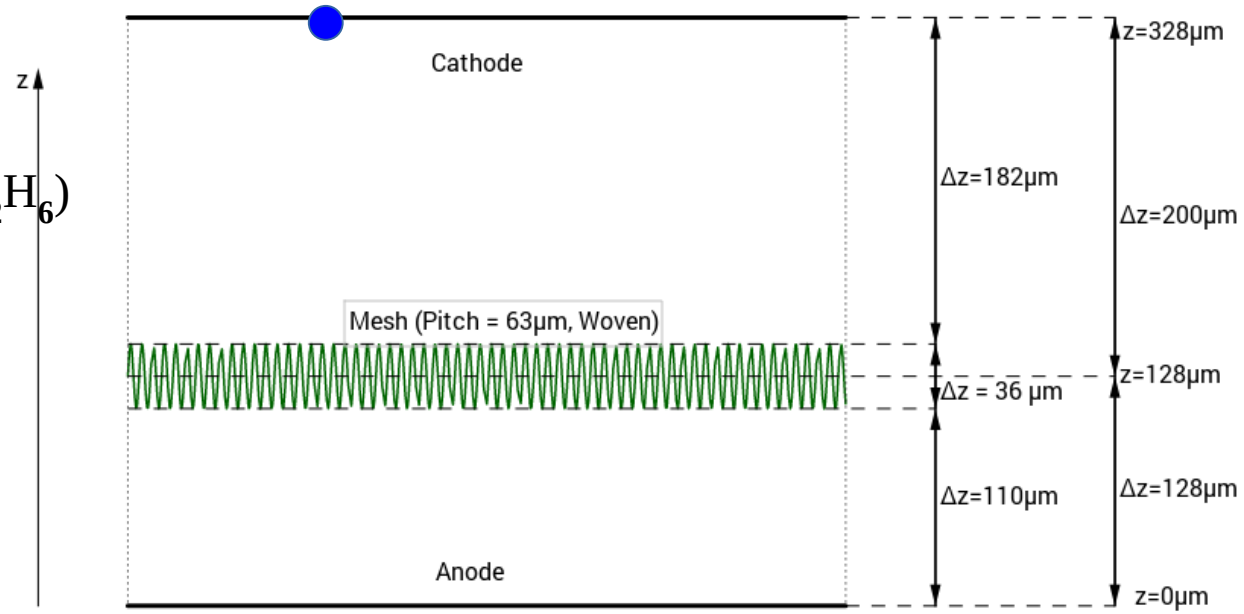

Anode volt age = 450 V
→ E = 35 kV/cm
Cathode voltage = 300-425 V
→ E in [15, 21] kV/cm

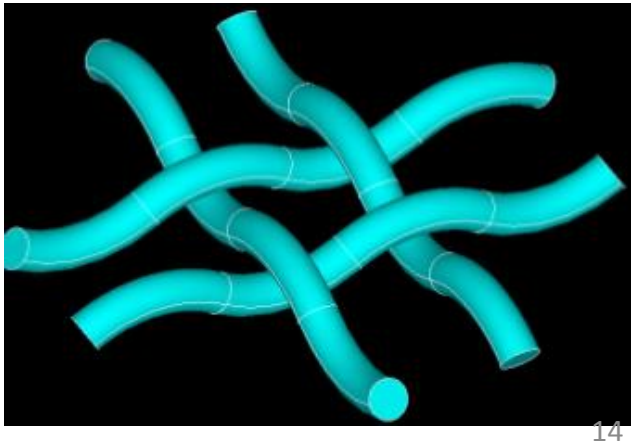

Describe the PICOSEC Response to a Single Photoelectrpn using Detailed Garfield++ Simulation including Penning Effect and the Electronics Response

An iterative method to determine the PICOSEC signal response (shape and amplitude distribution) to a single electron passing through the mesh and avalanching in the anode region

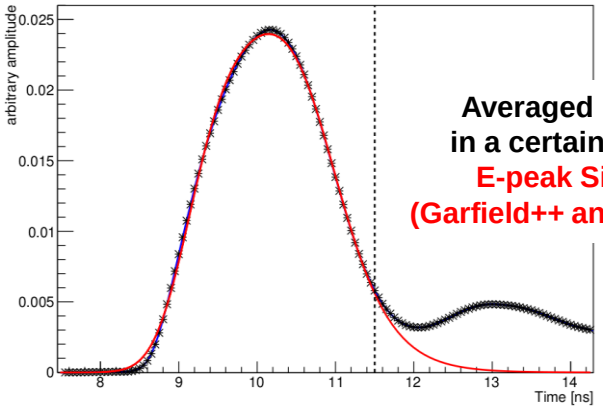

Averaged PICOSEC waveforms in a certain e-peak charge region
E-peak Simulation Prediction (Garfield++ and Electronics Response)

$(80\%\ Ne + 10\%\ CF_4 + 10\%\ C_2H_6)$

Determination of the COMPASS-gas Penning Transfer Rate by comparing the simulated to the experimental e-peak charge distribution and demanding the related normalization factor to be the same, independent of the operating voltages

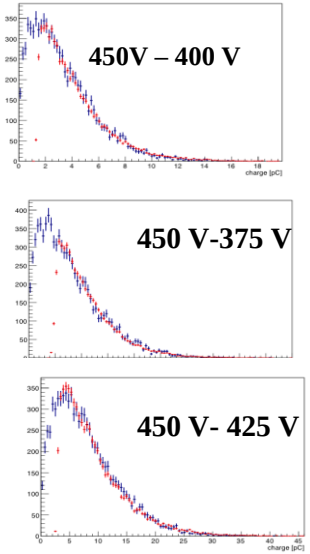

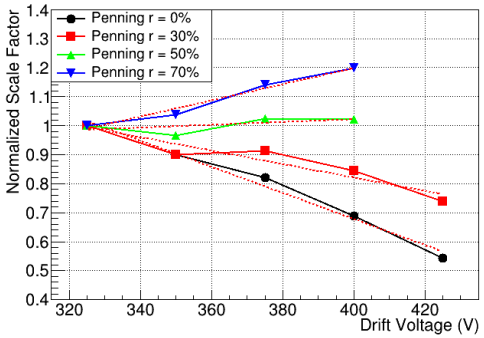

K. Paraschou, *"Study of the PICOSEC Micromegas Detector with Test Beam Data and Phenomenological Modelling of its Response"*, Master's Thesis, School of Physics, Aristotle University of Thessaloniki, https://ikee.lib.auth.gr/record/297707/ (2018).

There is a very good agreement between the “trimmed” Garfield++ simulations and the experimental data

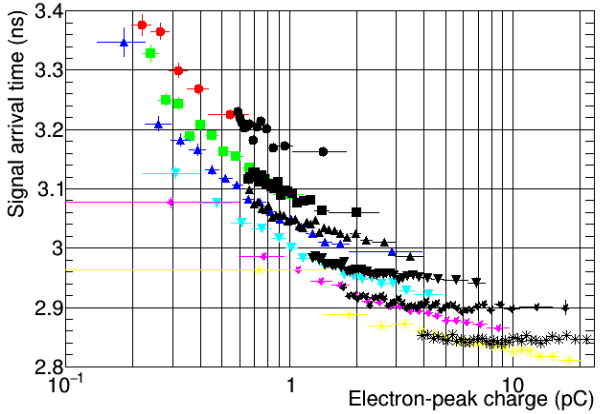

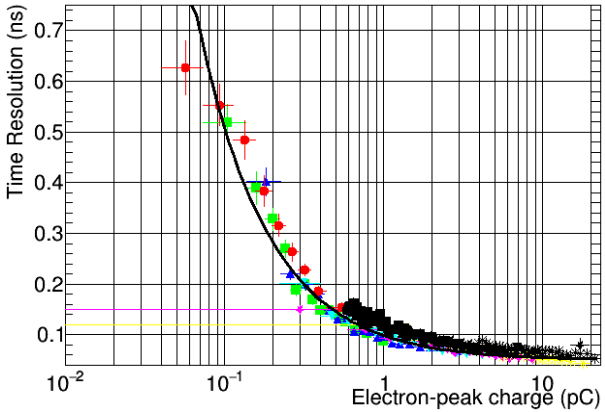

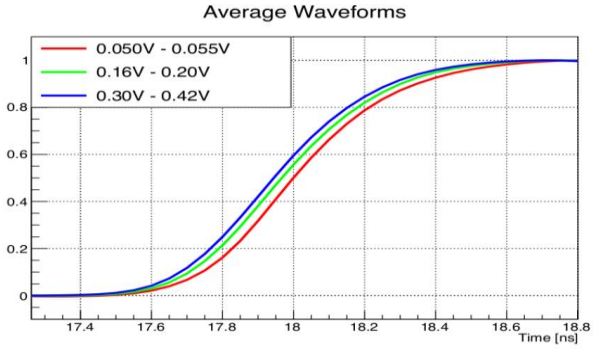

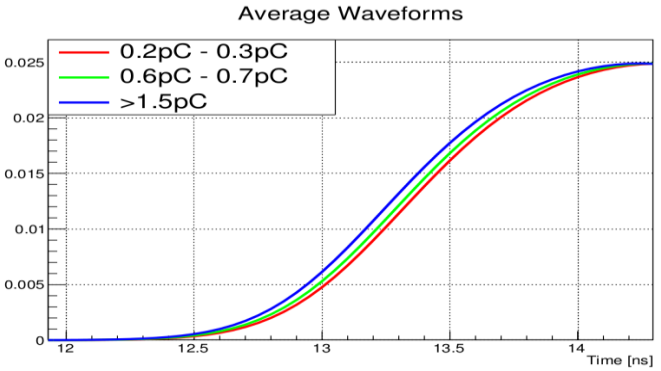

And all the behaviours we see in the data, are also seen in the simulation results.

Correspondence between microscopic and macroscopic infromation

In the GARFIELD++ simulated PICOSEC response to a single photoelectron, we have available:

Microscopic Information

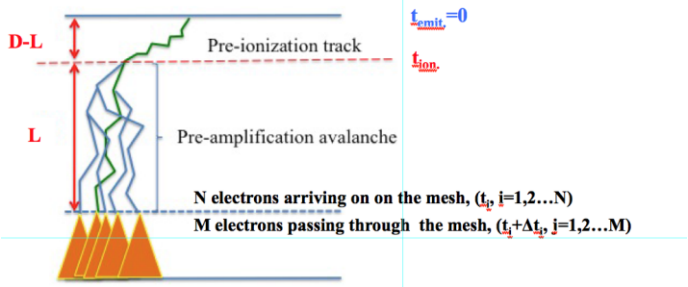

- **Total-time on the mesh:** $T_{tot} = \frac{1}{N}\sum_{i=1}^{N} t_i$
- **Total-time after the mesh:** $T_{a.m.} = \frac{1}{M}\sum_{i=1}^{M}(t_i + \Delta t_i)$
- **Photoelectron Transmission time:** $T_p = t_{ion}$
- **(Pre-amplification) Avalanche transmission time:** $T = \frac{1}{N}\sum_{i=1}^{N} t_i - t_{ion}$

Macroscopic Information –Exp. Observable

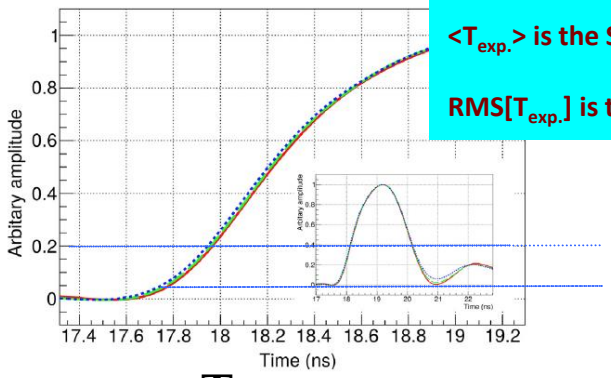

$T_{exp.}$

$T_{exp.}$ is a Random Variable

$\langle T_{exp.} \rangle$ is the S.A.T.

RMS[$T_{exp.}$] is the Timing Resolution

Correspondence of experimental Observables to Relevant Microscopic Variables

Sets of avalanches of a certain e-peak charge

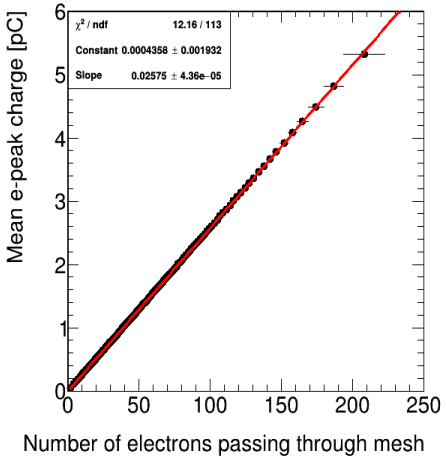

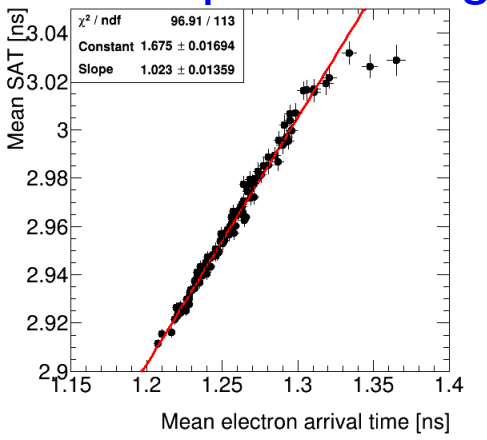

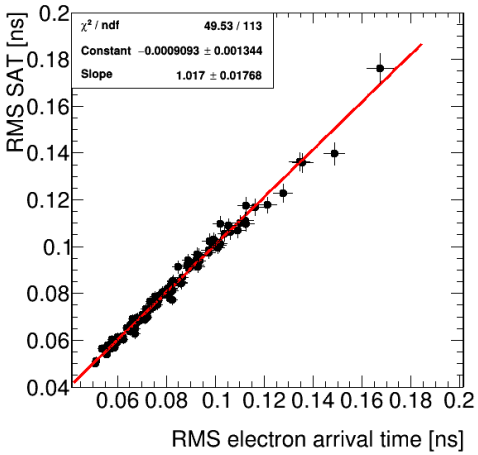

PICOSEC Timing Properties → statistical properties for pre-amplification electrons which passed through the mesh (population M, and time Tm)

Arrival times vs. avalanche length

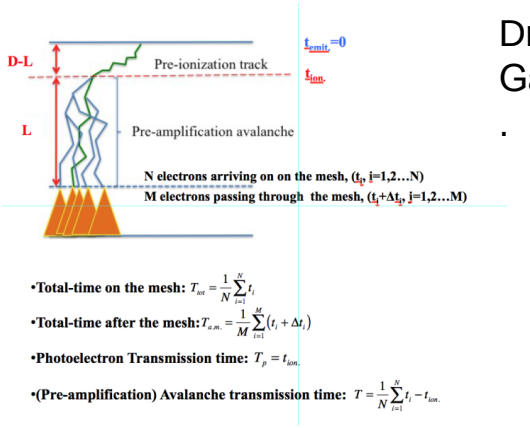

Drift times are expected to follow "inverse Gaussian" (= "Wald") distributions.

$$f(x;\mu,\lambda) = \left(\frac{\lambda}{2\pi x^3}\right)^{1/2} \exp\left[\frac{-\lambda(x-\mu)^2}{2\mu^2 x}\right]$$

- **The mean values of the transmission times depend linearly on the respective drift lengths.**

	Penning T. R. 0%	Penning T. R. 50%	Penning T. R. 100%
Photoelectron Drift Velocity (μm/ns)	156.8 ± 0.4	150.5 ± 0.8	142.2 ± 1.0
Avalanche Drift Velocity (μm/ns)	181.4 ± 0.5	184.8 ± 0.8	188.2± 0.9

The photoelectron drifts with less speed than the avalanche (as a whole) !!!

144.45 <L<144.75 μm

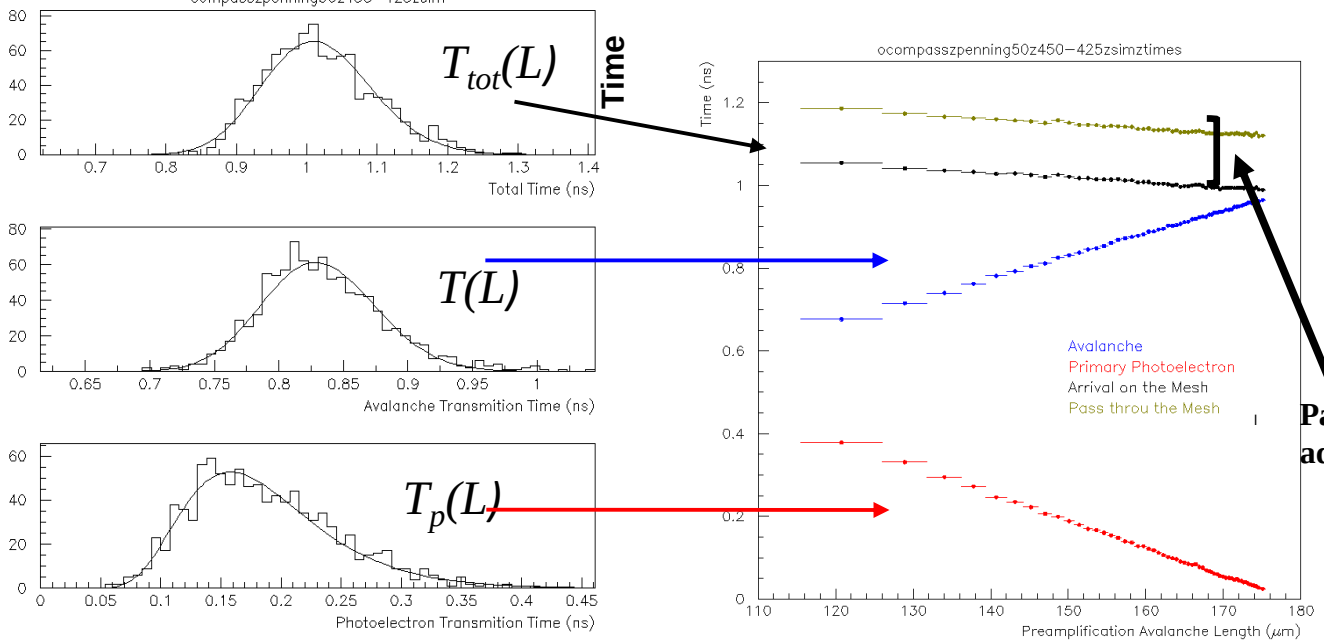

Passing through the mesh: just adds a constant time

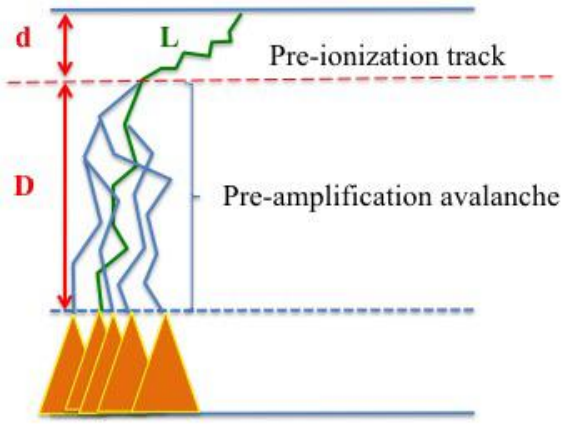

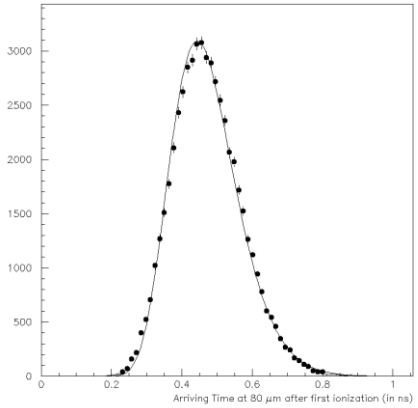

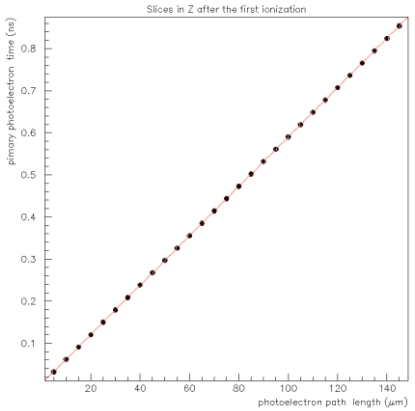

(left) The arriving-time distribution of an avalanche's electron at a longitudinal distance of 80μm from the start of the avalanche. (right) The mean drift times of an avalanche electron versus the corresponding drift distances.

	Penning T. R. 0%	Penning T. R. 50%	Penning T. R. 100%
Photoelectron Drift Velocity (μm/ns)	156.8 ± 0.4	150.5 ± 0.8	142.2 ± 1.0
Avalanche Drift Velocity (μm/ns)	181.4 ± 0.5	184.8 ± 0.8	188.2± 0.9
Electron in Avalanche Drift Velocity (μm/ns)	169.9± 0.2	170.4± 0.2	170.0 ± 0.2

An individual electron in the avalanche drifts slower than the avalanche as a whole !!! with a drift velocity independent of the Penning Transfer Rate !!!

Knowing already that the avalanche as a whole drifts faster than its' constituent electrons, we examine how much earlier it arrives to the mesh compared to what would be the case if it was drifting with the speed of the constituents

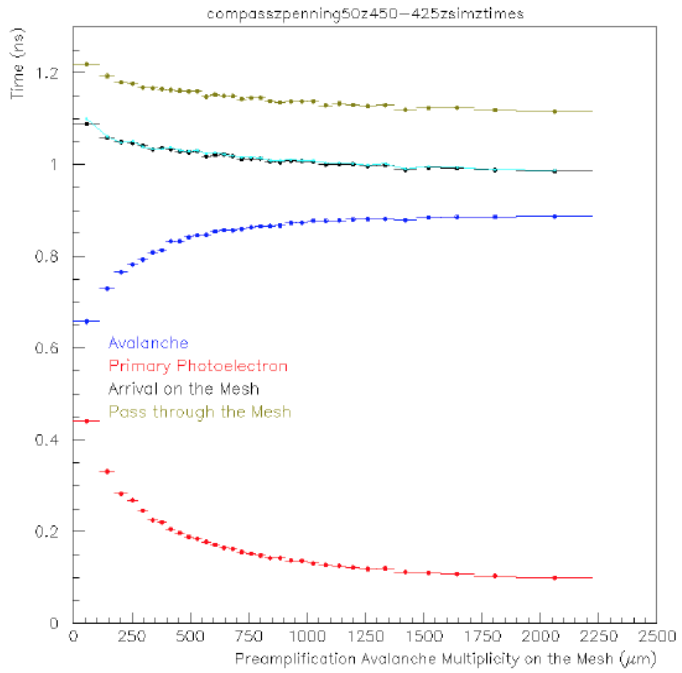

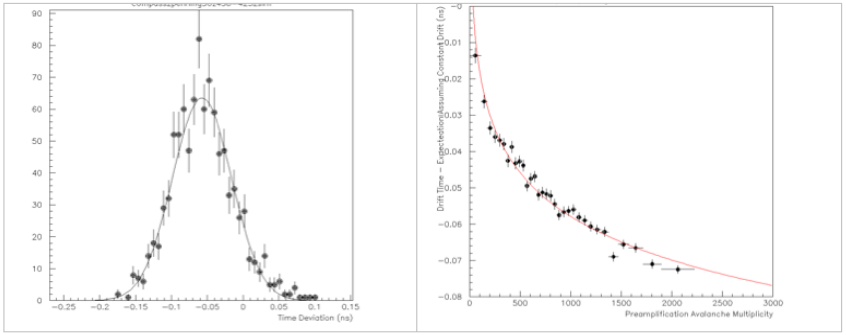

Figure 13: *(left) The distribution of the difference between: a) the time needed for an avalanche to reach the mesh, with electron multiplicities between 1003 and 1052 electrons on the mesh and b) the expected time assuming that the avalanche drift velocity equals to the drift velocity of a single electron in the avalanche. The solid curve represents a Gaussian fit. (right) The mean values of the above time deviations versus the corresponding electron multiplicities. The line represents a fit with the function defined in eq. (6), as it is described in the text.*

The time gain got the avalanche as a whole (relative to the individual constituents) depends logarithmically on its electron multiplicity !

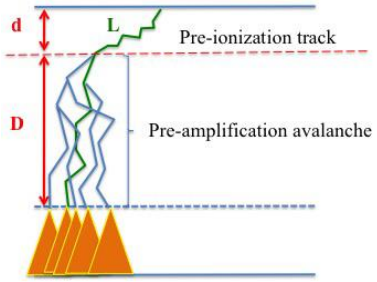

Timing Resolution as a Function of the Avalanche Length.

The time spread, which is related to the avalanche transmission is almost independent of the avalanche length!!

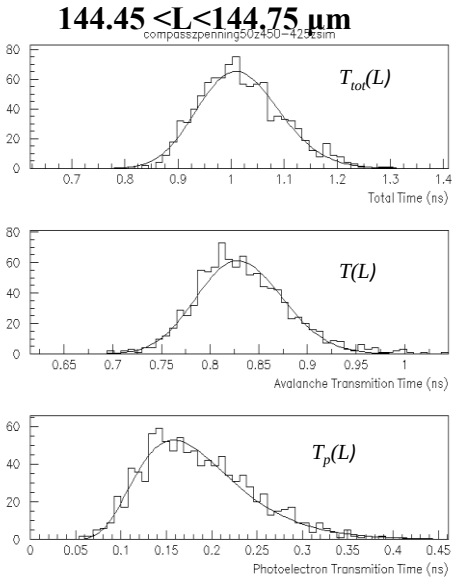

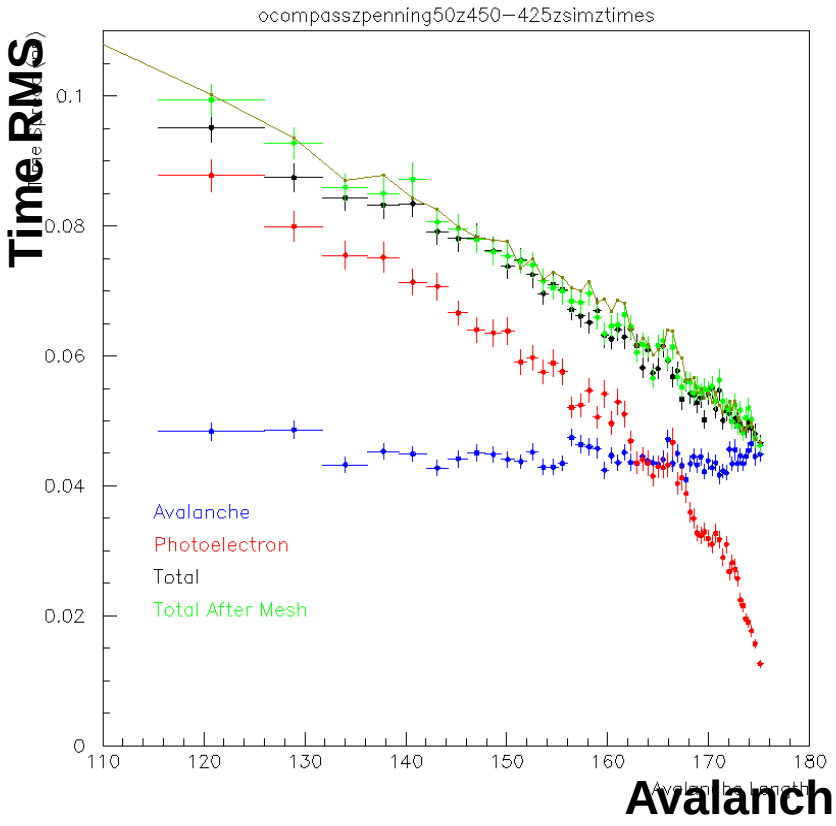

Avalanche length

1. Constant RMS for avalanche, no matter what it's length !!!
2. Photoelectron dominates time resolution, when it has enough drift length itself (large avalache length → small photoelectron drift length)
3. Avalanche and photoelectron contributions are statistically independent (at a given length the total RMS is the quadrature sum)
4. The passage through the mesh does not increase the time spread (black points on top of green points) when the drift voltage is high !!!

Timing Resolution as a Function of the Number of Pre-amplification Electrons.

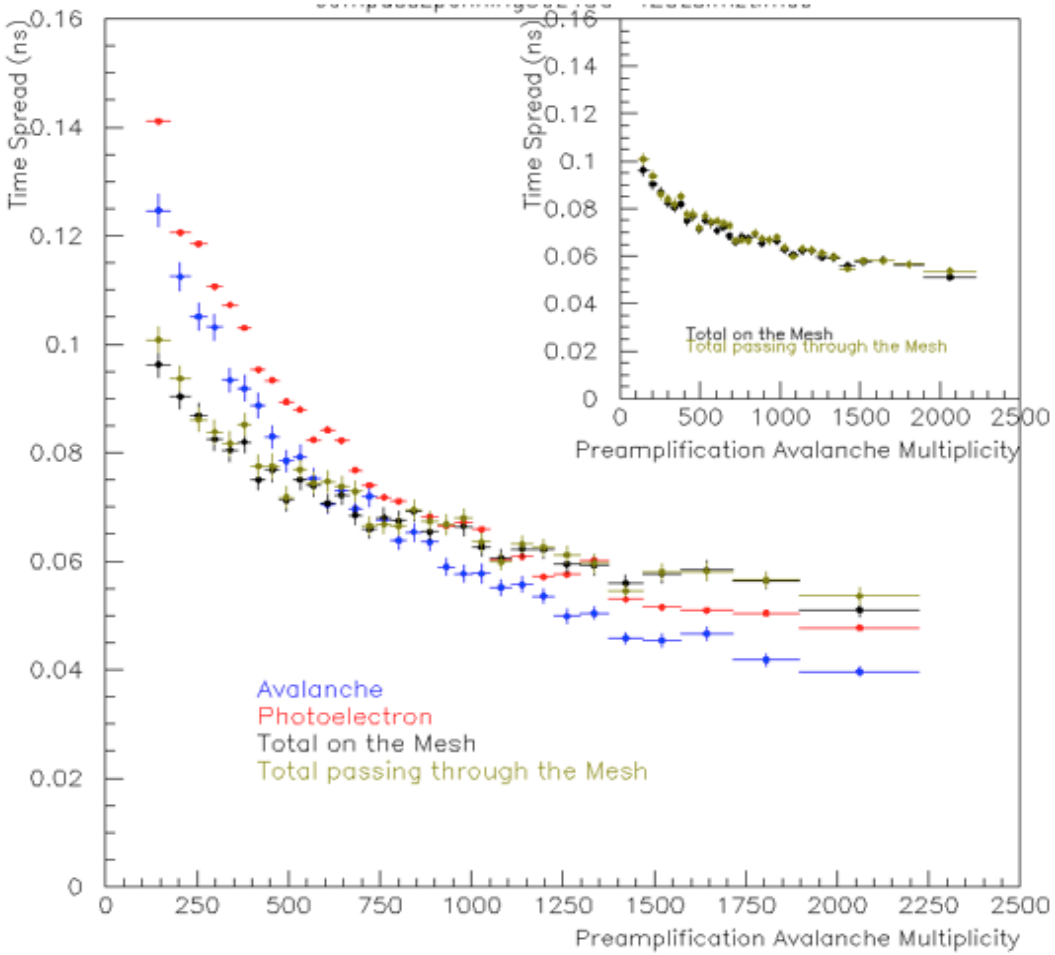

1. the photoelectron & avalanche contributions to the total time spread are statistically, heavily correlated How comes this correlation?

2. The transmission through the mesh (~25%), at high drift voltages, does not affect the resolution of the PICOSEC !!!.

Summarize the effect of the mesh

- **The mesh transparency is almost constant (~25%), independent of the drift and anode voltages**
- **The transmision through mesh adds a time delay, independent of the pre-amplification avalanche multiplicity**
- **At lower drift voltages the mesh adds a spread which drops with the pre-amplification avalanche population !!!**
- **At higher drift voltages the mesh does not affect the time spread !!!**

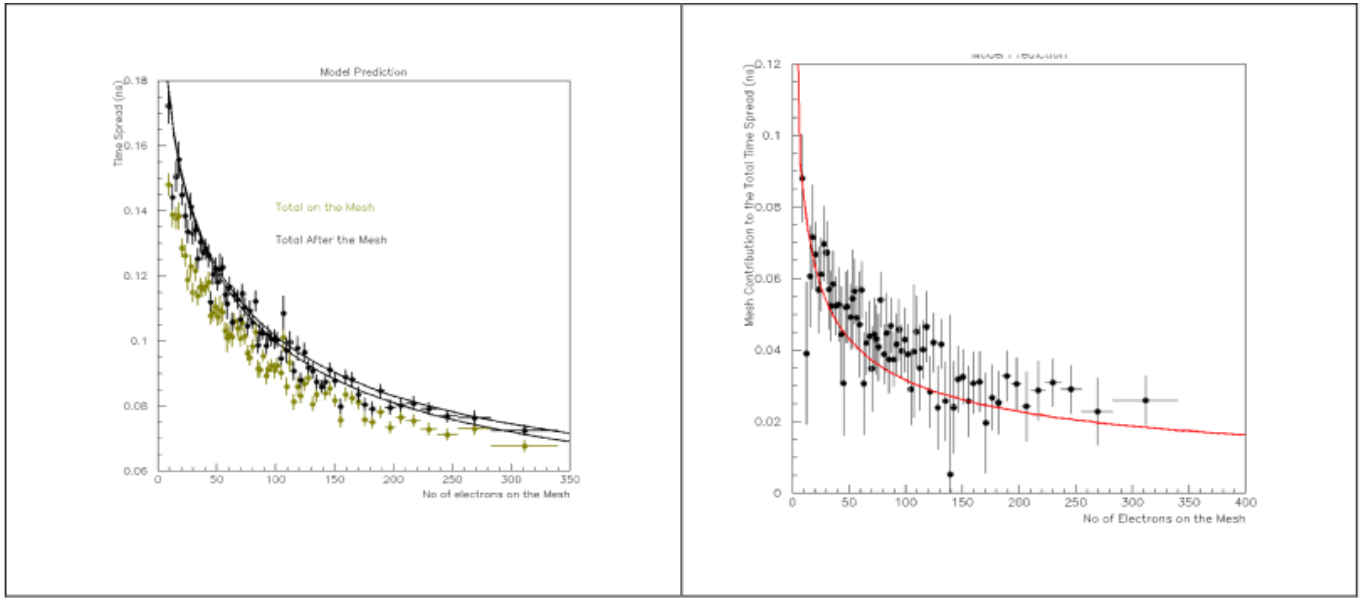

Figure 31: *(left) Total-time spread versus the number of electrons on the mesh, evaluated from GARFIELD++ simulations, on (golden) and after (black) passing the mesh in comparison with the prediction of eq. (31). (right) The prediction (red line) of the mesh effect on the timing resolution of eq. (32) is compared to the simulation results (black points). The anode and the drift voltages are 450 V and 350 V, respectively.*

GARFIELD++ adds with more questions than answers

GARFIELD++ predicts that:

1. The avalanche drifts faster than the photoelectron before ionization , $V_a > V_p$. *(It explains qualitatively the dependence of the SAT on the e-peak size, i.e. the SAT, relative to the photoelectron emission, decreases linearly with the avalanche length, longer avalanches produce more electrons)*
2. The avalanche electron drifts faster than the photoelectron, $V_{ea} > V_p$ *(This is due to more frequent inelastic collisions in the avalanche*
3. The avalanche drifts faster than its constituent avalanche electrons, $V_a > V_{ea}$. *(WHY? and HOW?)*
4. The avalanche time, i.e. the time taken by an avalanche to drift a certain length L, also depends explicitly on the electron multiplicity at L *(WHY? and HOW?)*
5. The PICOSEC timing resolution depends strongly on the longitudinal diffusion. The variance of the photoelectron time and of the avalanche electron transmission time depend, as expected, on the drift length. However, the variance of the avalanche time is almost constant, independent of the respective transmission length. *(WHY? and HOW?)*
6. The photoelectron time and the avalanche time, when they are expressed in terms of the multiplicity of the pre-amplification electrons, are mutually, heavily correlated. *(How this correlation affects the observed dependence of the PICOSEC Timing Resolution? How this correlation comes?)*
7. The transport of the pre-amplification electrons through the mesh adds to the SAT a constant time delay, which, for any set of voltage settings, is independent of the signal size *(WHY?)*
8. The passage through the mesh depletes the number of pre-amplification electrons by a factor of 4 (in all the voltage settings considered in this study). At high drift voltages (e.g. 425V) this depletion leaves practically unaffected the PICOSEC resolution. However, at lower drift voltages (e.g <375 V) the timing resolution worsens, even if the mesh transparency remains the same. This effect depends on the pre-amplification avalanche multiplicity (and length) in a specific way. *(WHY? and HOW?)*

Understanding the Physics of Precise Timing

A model inspired by the effect of quenchers in noble gasses:

Electrons in Ar/CO_2 at E=1 kV/cm

Plots from Rob Veenhof

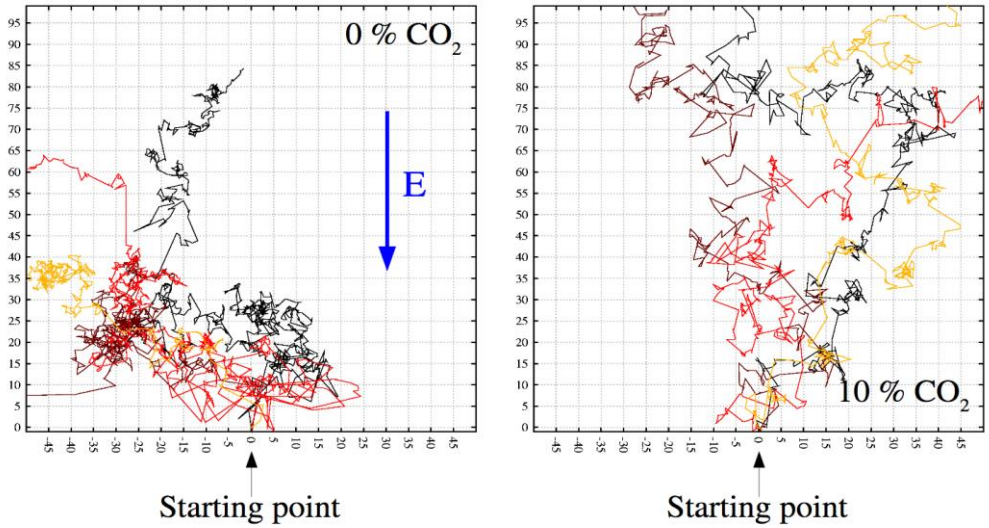

Scatterings WITH some significant energy losses

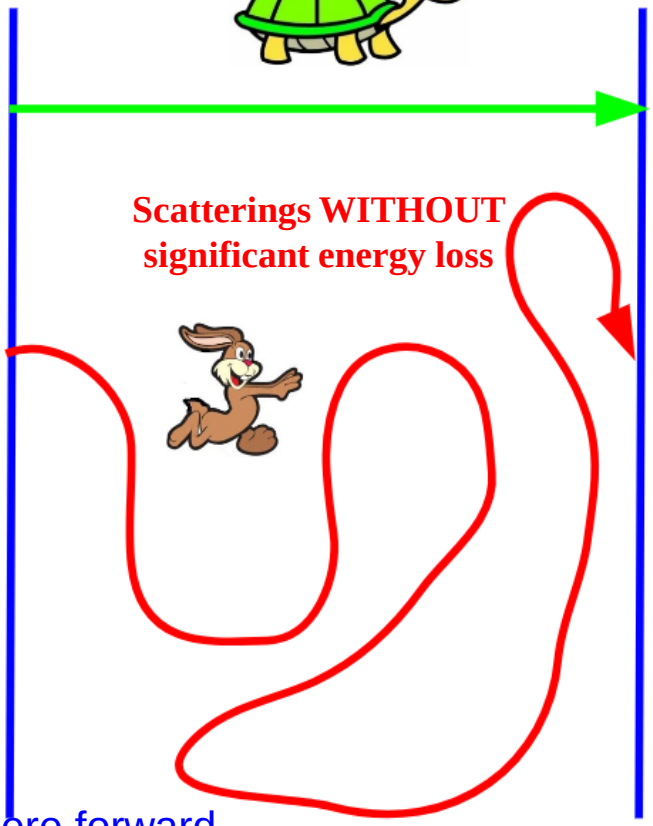

The more quencher we have, the faster we arrive somewhere forward.

The average forward speed of the very energetic rabbit is lower than the turtle!

Like a bouncing ball:

if only elastically scattered, it goes backward with a lot of energy and it looses time before the Electric field brings it back to forward motion again!

So, with an inelastic collision, the photoelectron gains time compared to an elastic collisions! →

Modeling the Timing Characteristics of the PICOSEC Micromegas Detector

J. Bortfeldt[b], F. Brunbauer[b], C. David[b], D. Desforge[a], G. Fanourakis[e], J. Franchi[b], M. Gallinaro[g], F. García[k], I. Giomataris[a], T. Gustavsson[i], C. Guyot[a], F.J. Iguaz[a], M. Kebbiri[a], K. Kordas[d], P. Legou[a], J. Liu[c], M. Lupberger[b], O. Maillard[a], I. Manthos[d], H. Müller[b], V. Niaouris[d], E. Oliveri[b], T. Papaevangelou[a], K. Paraschou[d], M. Pomorski[j], B. Qi[c], F. Resnati[b], L. Ropelewski[b], D. Sampsonidis[d], T. Schneider[b], P. Schwemling[a], L. Sohl[a], M. van Stenis[b], P. Thuiner[b], Y. Tsipolitis[f], S.E. Tzamarias[d,*], R. Veenhof[h,l,m], X. Wang[c], S. White[b], Z. Zhang[c], Y. Zhou[c]

arXiv:1901.10779v1 [physics.ins-det]

The Model

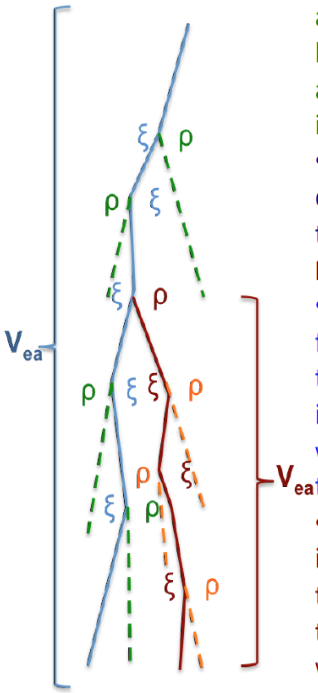

•An ionizing electron in the avalanche, every time it ionizes, will gain a time ξ_l relative to an electron that undergoes elastic scatterings only.

• Any newly produced electron by ionization starts with low energy; at the start of its path, it suffers less delay due to elastic backscattering compared to its parent. Therefore, the model assumes that such a newly produced electron will gain, relative to its parent, a time-gain ρ_l.

• The parameters ξ_l and ρ_l should follow a joint probability distribution determined by the physical process of ionization and the respective properties of interacting molecules.

Model Approximations

•The collective effect of time-gains ξ_l is a change in drift velocity from V_p, which is the photoelectron drift velocity before ionization, to an effective drift velocity V_{ea}, which is the drift velocity of an ionizing electron in the avalanche. By taking V_{ea} to be the drift velocity of any electron in the avalanche, the energy-loss effect on the drift of the parent electron has been taken into account.

•When a new electron is produced in the avalanche, through ionization, it will gain time ρ_l, at its production, which it is assumed to follow a distribution with mean value ρ and variance w^2. From that moment onwards, this new electron propagates with drift velocity V_{ea}, as any other existing electron in the avalanche.

Modeling the Timing Characteristics of the PICOSEC Micromegas Detector

J. Bortfeldt[b], F. Brunbauer[b], C. David[b], D. Desforge[a], G. Fanourakis[e], J. Franchi[b], M. Gallinaro[g], F. García[k], I. Giomataris[a], T. Gustavsson[i], C. Guyot[a], F.J. Iguaz[a], M. Kebbiri[a], K. Kordas[d], P. Legou[a], J. Liu[c], M. Lupberger[b], O. Maillard[a], I. Manthos[d], H. Müller[b], V. Niaouris[d], E. Oliveri[b], T. Papaevangelou[a], K. Paraschou[d], M. Pomorski[j], B. Qi[c], F. Resnati[b], L. Ropelewski[b], D. Sampsonidis[d], T. Schneider[b], P. Schwemling[a], L. Sohl[a], M. van Stenis[b], P. Thuiner[b], Y. Tsipolitis[f], S.E. Tzamarias[d,*], R. Veenhof[h,l,m], X. Wang[c], S. White[b], Z. Zhang[c], Y. Zhou[c]

arXiv:1901.10779v1 [physics.ins-det]

The Model

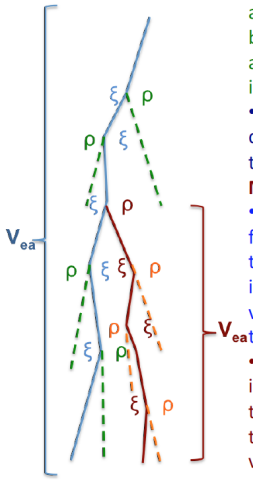

•An ionizing electron in the avalanche, every time it ionizes, will gain a time ξ_i relative to an electron that undergoes elastic scatterings only.

• Any newly produced electron by ionization starts with low energy; at the start of its path, it suffers less delay due to elastic backscattering compared to its parent. Therefore, the model assumes that such a newly produced electron will gain, relative to its parent, a time-gain ρ_i.

• The parameters ξ_i and ρ_i should follow a joint probability distribution determined by the physical process of ionization and the respective properties of interacting molecules.

Model Approximations

•The collective effect of time-gains ξ_i is a change in drift velocity from V_p, which is the photoelectron drift velocity before ionization, to an effective drift velocity V_{ea}, which is the drift velocity of an ionizing electron in the avalanche. By taking V_{ea} to be the drift velocity of any electron in the avalanche, the energy-loss effect on the drift of the parent electron has been taken into account.

•When a new electron is produced in the avalanche, through ionization, it will gain time ρ_i, at its production, which it is assumed to follow a distribution with mean value ρ and variance w^2. From that moment onwards, this new electron propagates with drift velocity V_{ea}, as any other existing electron in the avalanche.

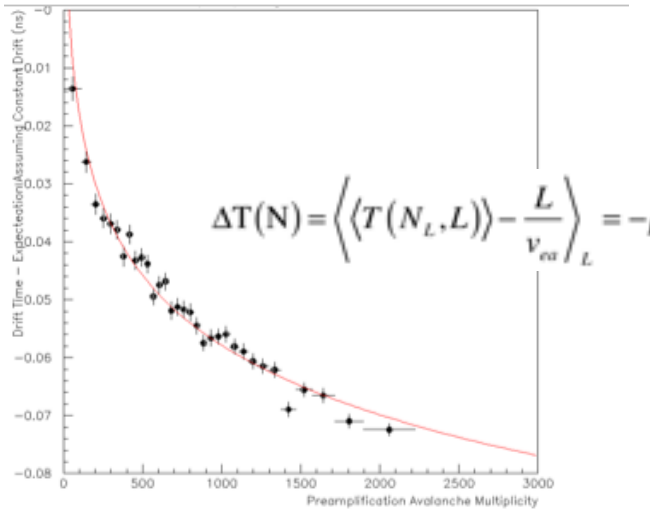

$$\Delta T(N) = \left\langle \langle T(N_L, L) \rangle - \frac{L}{v_{ea}} \right\rangle_L = -\rho \ln N_L + C$$

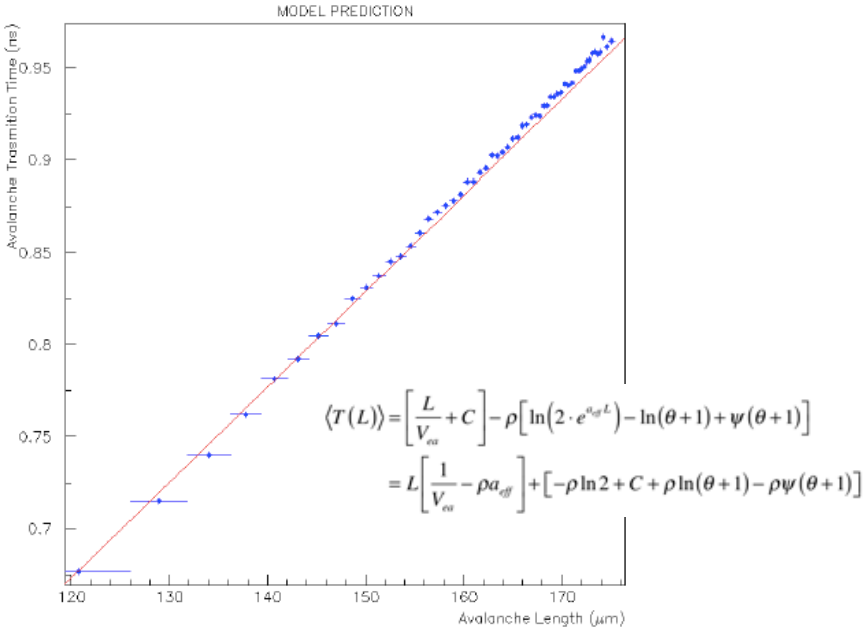

$$\langle T(L) \rangle = \left[\frac{L}{V_{ea}} + C \right] - \rho \left[\ln\left(2 \cdot e^{a_{eff} L}\right) - \ln(\theta+1) + \psi(\theta+1) \right]$$

$$= L\left[\frac{1}{V_{ea}} - \rho a_{eff} \right] + \left[-\rho \ln 2 + C + \rho \ln(\theta+1) - \rho \psi(\theta+1) \right]$$

Very successful in predicting the Resolution vs Avalanche Length Dependence

The Input Parameters are the gas properties, i.e. single-e drift parameters, Townsend coefficient, Polya parameters

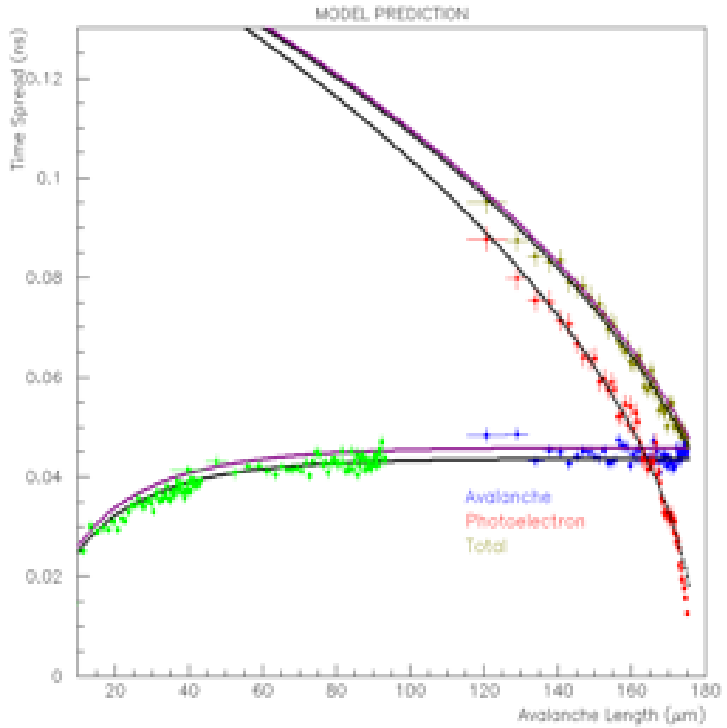

$$V\left[T_p(L)\right] = (D-L)\cdot\sigma_p^2 + \Phi$$

$$V\left[T(L)\right] = \frac{(\theta+1)}{2\theta}\left[\sigma_0^2 + w^2 a_{eff}\right]\frac{1-\exp\left(-a_{eff}\cdot L\right)}{a_{eff}}$$

$$V\left[T_{tot}(L)\right] = V\left[T(L)\right] + V\left[T_p(L)\right]$$
$$= \frac{(\theta+1)}{2\theta}\left[\sigma_0^2 + w^2 a_{eff}\right]\frac{1-\exp\left(-a_{eff}\cdot L\right)}{a_{eff}} + (D-L)\cdot\sigma_p^2 + \Phi$$

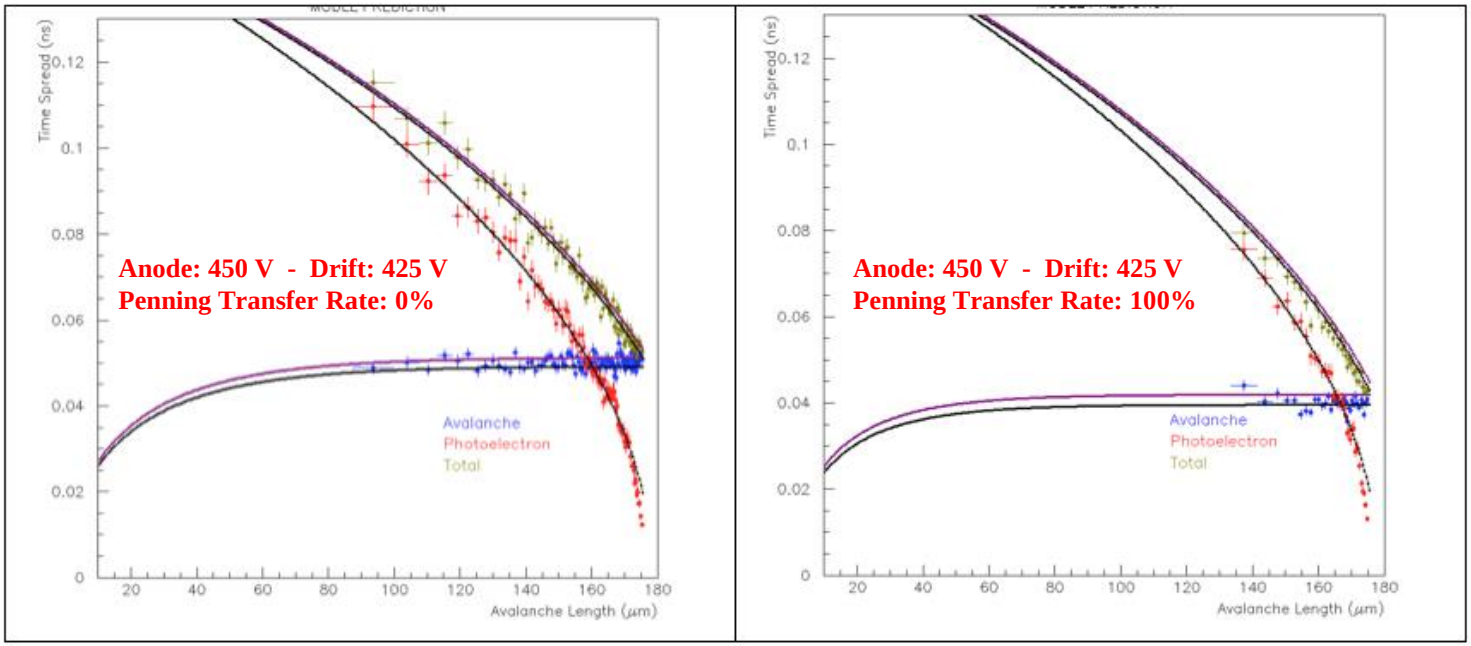

Anode: 450 V - Drift: 325 V
Penning Transfer Rate: 50%

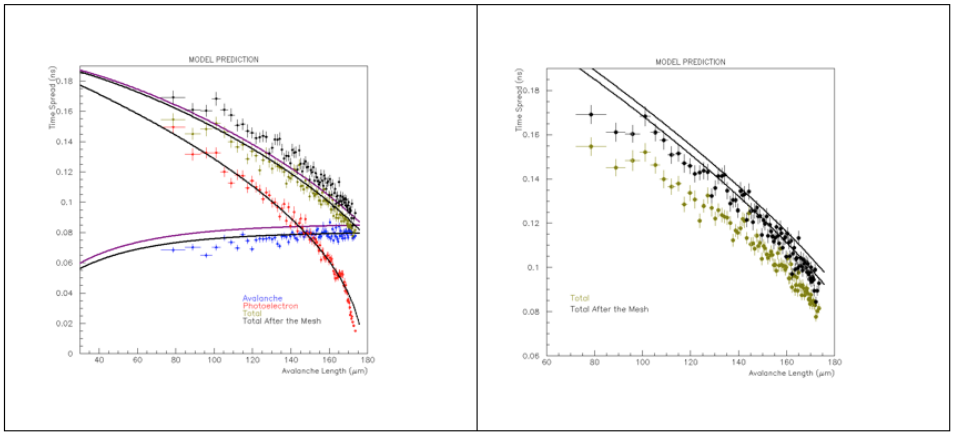

Anode: 450 V - Drift: 350 V
Penning Transfer Rate: 50%

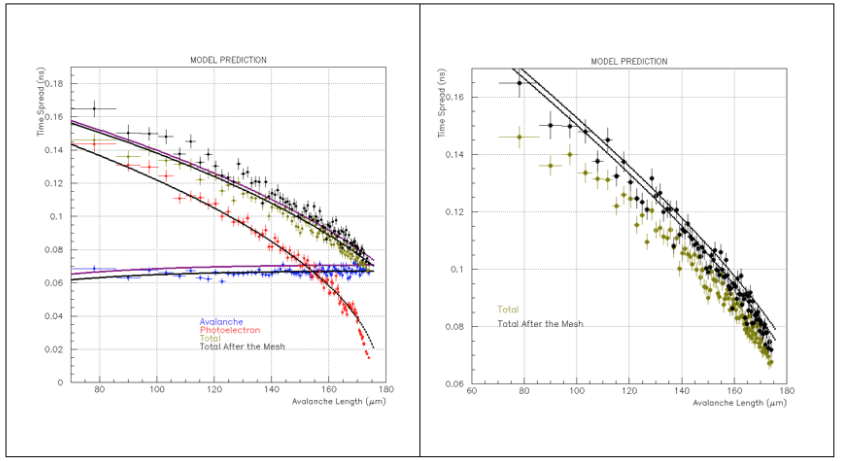

Very successful in predicting the Resolution vs Avalanche Multiplicity Dependence

Anode: 450 V - Drift: 425 V
Penning Transfer Rate: 50%

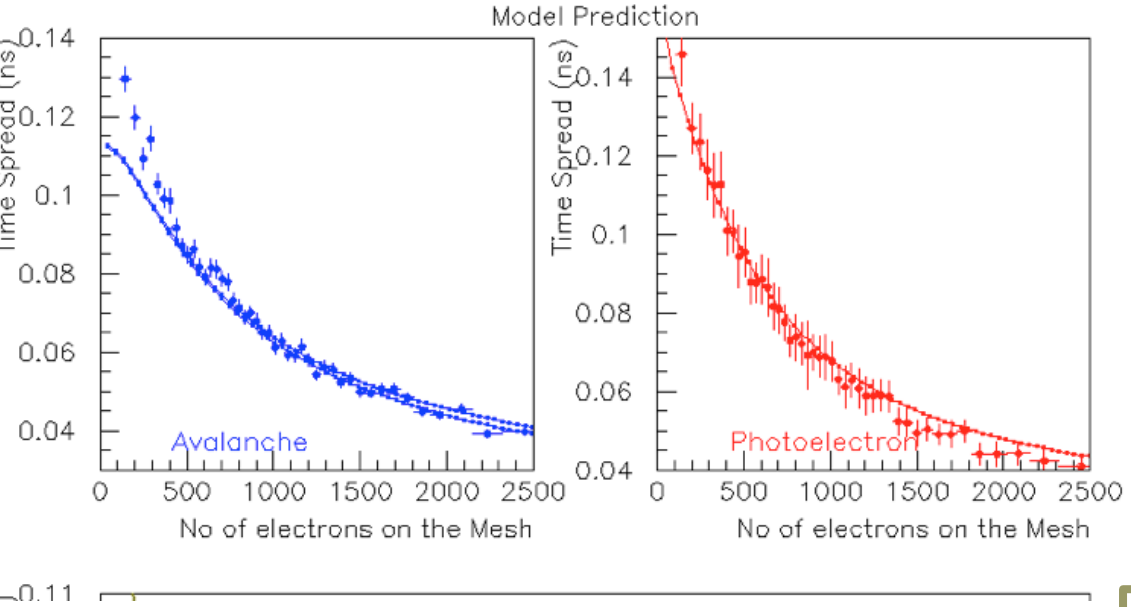

$$\langle V(N)\rangle = \int_{x_1}^{x_2} \langle V(L)\rangle_{n(L)=N} \cdot G(L|N)\,dL + \int_{x_1}^{x_2} \langle T(N,L)\rangle^2 \cdot G(L|N)\,dL - \left[\int_{x_1}^{x_2} \langle T(N,L)\rangle \cdot G(L|N)\,dL\right]^2$$

$$\langle V_p(N)\rangle = \int_{x_1}^{x_2} V_p(L) \cdot G(L|N)\,dL + \int_{x_1}^{x_2} T_p^2(L) \cdot G(L|N)\,dL - \left[\int_{x_1}^{x_2} T_p(L) \cdot G(L|N)\,dL\right]^2$$

$$\langle V_{tot}(N)\rangle = \int_{x_1}^{x_2} \left[V_p(L) + \langle V(L)\rangle_{n(L)=N}\right] \cdot G(L|N)\,dL + \int_{x_1}^{x_2} \left[\langle T(N,L)\rangle + T_p(L)\right]^2 \cdot G(L|N)\,dL - \left[\int_{x_1}^{x_2} \left[\langle T(N,L)\rangle + T_p(L)\right] \cdot G(L|N)\,dL\right]^2$$

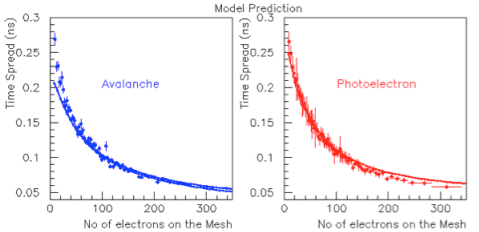

Anode: 450 V - Drift: 350 V
Penning Transfer Rate: 50%

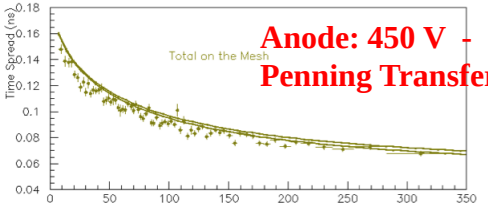

Very successful in predicting the effect of the *"transmission through the mesh"* on the Timing Resolution

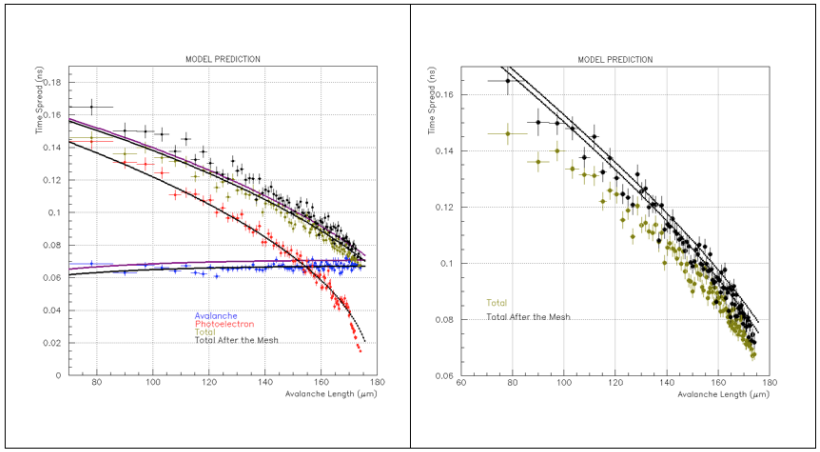

Figure 29: *(left) Time spreads versus the avalanche length. The solid lines represent the model predictions. (right) Time spreads of avalanche transmission times reaching (golden) and passing through (black) the mesh. The solid lines correspond to the model prediction when taking into account the mesh effect. The anode and the drift voltages are 450 V and 350 V, respectively.*

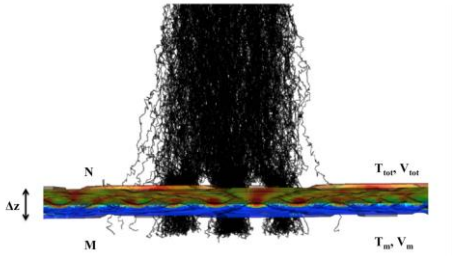

$$\langle V_m(L)\rangle = \frac{\theta+1}{2\theta}\exp\left[-a_{eff}L\right]\cdot\left[\sigma_0^2\cdot L\left(\frac{1}{tr}-1\right)+\frac{\delta^2}{tr}\right]+\langle V_{tot}(L)\rangle$$

$$\Delta V(L) = \langle V_m(L)\rangle - \langle V_{tot}(L)\rangle = \frac{\theta+1}{2\theta}\exp\left[-a_{eff}L\right]\cdot\left[\sigma_0^2\cdot L\left(\frac{1}{tr}-1\right)+\frac{\delta^2}{tr}\right]$$

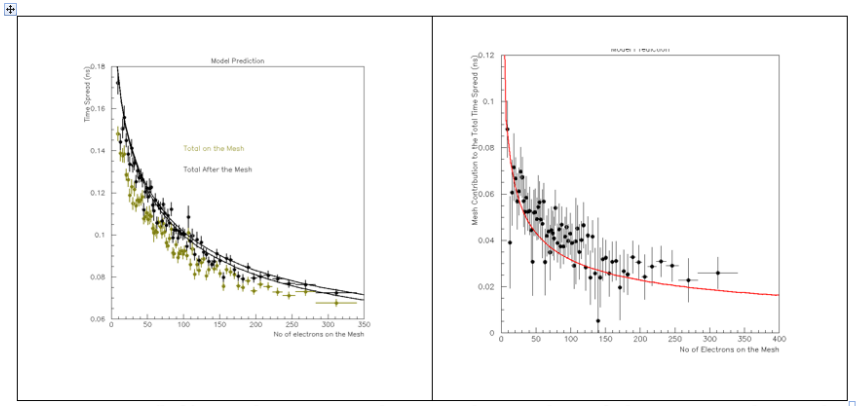

Figure 31: *(left) Total-time spread versus the number of electrons on the mesh, evaluated from GARFIELD++ simulations, on (golden) and after (black) passing the mesh in comparison with the prediction of eq. (31). (right) The prediction (red line) of the mesh effect on the timing resolution of eq. (32) is compared to the simulation results (black points). The anode and the drift voltages are 450 V and 350 V, respectively.*

$$\langle V_m(N)\rangle = \frac{1}{N}\left[\sigma_0^2\cdot\langle L(N)\rangle\left(\frac{1}{tr}-1\right)+\frac{\delta^2}{tr}\right]+\langle V_{tot}(N)\rangle$$

$$\Delta V(N) = \langle V_m(N)\rangle - \langle V_{tot}(N)\rangle = \frac{1}{N}\left[\sigma_0^2\cdot\langle L(N)\rangle\left(\frac{1}{tr}-1\right)+\frac{\delta^2}{tr}\right]$$

With the extra assumption that all the relevant time distributions can be expressed as inverse Gaussians, the Model describes stochastically all the timing characteristics of the PICOSEC detector in a very good agreement with the GARFIELD++ detail simulation

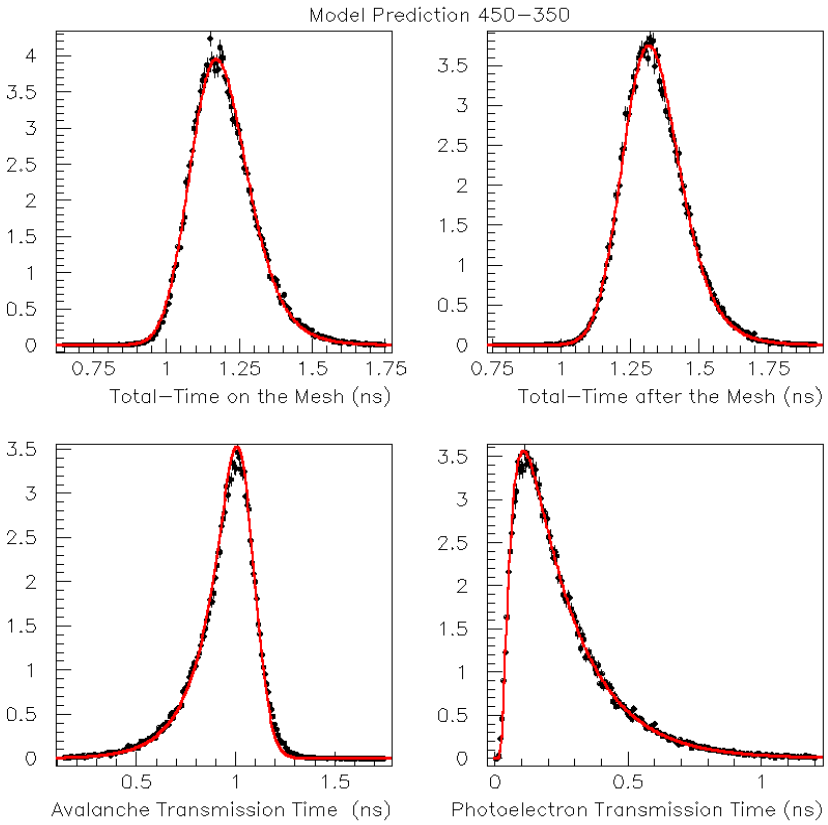

Conclusions

A simple phenomenological model has been developed which predict the timing characteristics of the PICOSEC signal, in terms of fundamental variables compiled in Table 8 for several drift voltage settings, in a very good agreement with results based on GARFIELD++ detailed simulations

TABLE 8: Values of the parameters used by the model

Penning Transfer Rate	**50%**				
Anode Voltage	**450 V**				
Drift Voltage	**325 V**	**350 V**	**375 V**	**400 V**	**425 V**
a ($10^{-2}\mu m^{-1}$)	3.607 ± 0.018	4.400 ± 0.020	5.208 ± 0.027	6.069 ± 0.027	6.950 ± 0.032
a_{eff} ($10^{-2}\mu m^{-1}$)	2.215± 0.001	2.629± 0.001	3.055 ± 0.001	3.484 ± 0.001	3.912 ± 0.001
θ	2.698± 0.142	2.906± 0.154	3.037 ± 0.162	3.313 ± 0.179	3.645 ± 0.191
V_{ea}^{-1} (10^{-3}ns/μm)	7.311± 0.003	6.877± 0.003	6.509 ± 0.002	6.173 ± 0.002	5.866 ± 0.004
V_p^{-1} (10^{-3}ns/μm)	8.065± 0.026	7.678± 0.026	7.266 ± 0.028	6.923 ± 0.028	6.643 ± 0.031
d_{off} (10^{-2}ns)	-3.831 ± 0.084	-3.437 ± 0.082	-2.883 ± 0.075	-2.678 ± 0.068	-2.364 ± 0.079
ρ (10^{-2}ns)	3.570± 0.054	2.769± 0.027	2.489 ± 0.030	2.185 ± 0.028	1.725 ± 0.045
C (10^{-2}ns)	8.059 ± 0.218	6.840 ± 0.117	7.668 ± 0.166	7.778 ± 0.196	6.001 ± 0.216
σ_p^2 ($10^{-4}ns^2/\mu m$)	2.137± 0.054	1.908± 0.046	1.662± 0.053	1.554± 0.050	1.380± 0.063
Φ ($10^{-4}ns^2$)	-9.967 ± 2.417	-7.936 ± 1.395	-6.239 ± 1.607	-7.525 ± 1.343	-5.622 ± 1.284
σ_0^2 ($10^{-4}ns^2/\mu m$)	2.094 ± 0.005	1.778± 0.003	1.543± 0.004	1.341± 0.003	1.175± 0.004
tr	0.244± 0.009	0.248± 0.044	0.238± 0.011	0.251± 0.009	0.247± 0.009
δ (10^{-2}ns)	7.217 ± 0.034	6.871 ± 0.032	6.607 ± 0.031	6.305 ± 0.030	5.938 ± 0.040
Control Parameters					
x_1 (μm)	0	0	0	0	0
x_2 (μm)	164	167	174	174	172
w/ρ	1	1	1	1	1
D (μm)	182	182	182	182	182
Nmax	350	500	1250	1750	3500

Towards a robust detector

#1 robust anode
#2 robust photocathode

I. Maniatis talk

Best resolution was at voltages which give high currents on anode: robust anode

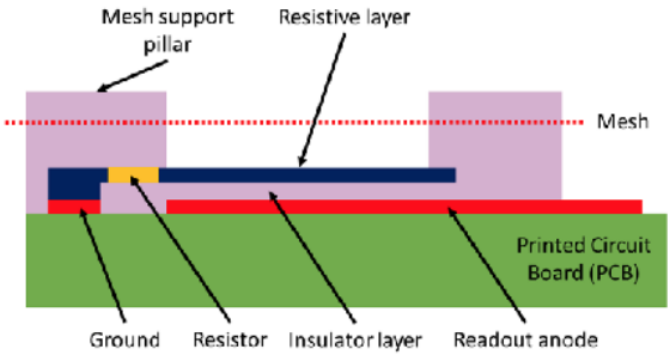

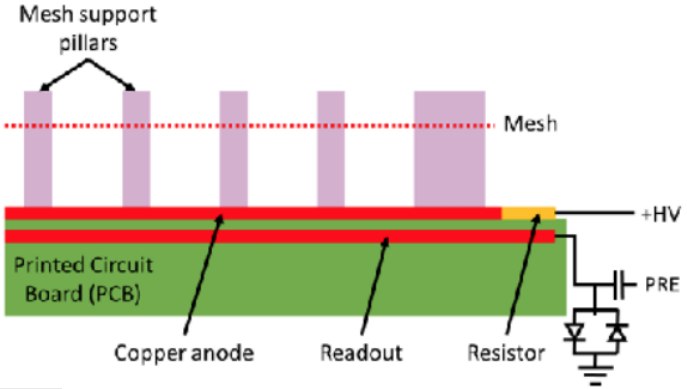

Readout beneath resistive layer: picks up signal from above

Copper Layer to HV via resistor; Readout "floating"

Resistive strip grounded

Developed in the MAMA project

Resistive readouts operate stably at high gain in neutron fluxes of 10^6 Hz/cm^2.

T. Alexopoulos *et al.*, *NIMA* **640** (2011) 110-118.

Non resistive ← MAMA results → With resistive strip

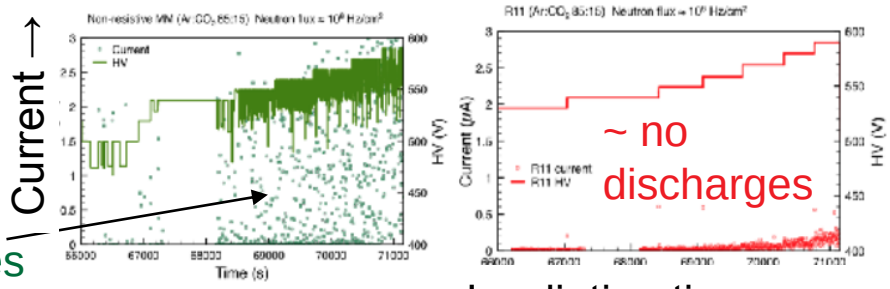

Beam results with protected anodes

Time resolution

Resistive strips

σ = 41 ps

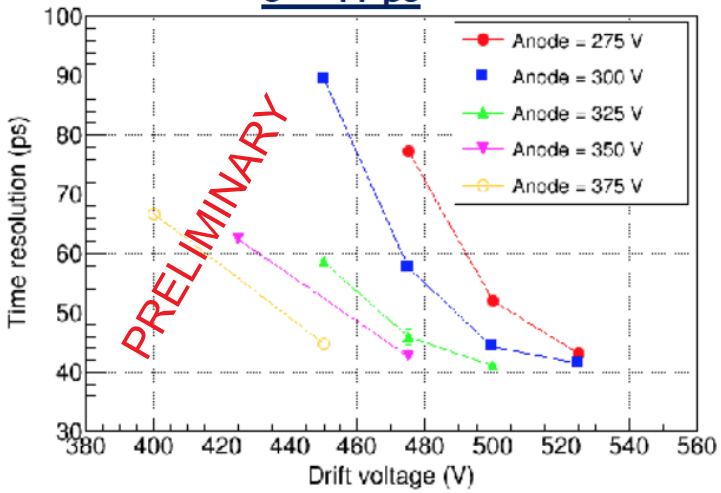

Floating strips

σ = 28 ps

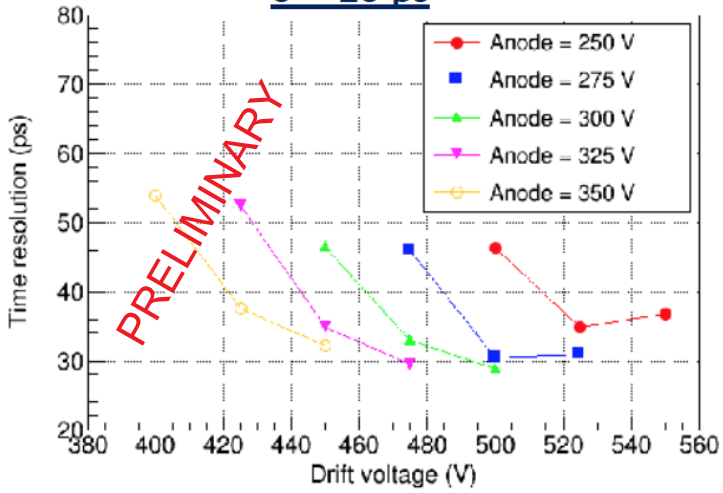

PRELIMINARY

- Values not far from the Picosec bulk readout.
  - **Resistive strips:** 41 ps (10 MΩ/□), 35 ps (300 kΩ/□).
  - **Floating strips:** 28 ps (25 MΩ).

Best resolution was at voltages which give high ion backflow? robust photocathode

Best time resolution (24ps for MIPs) for CsI photocathode, but not robust

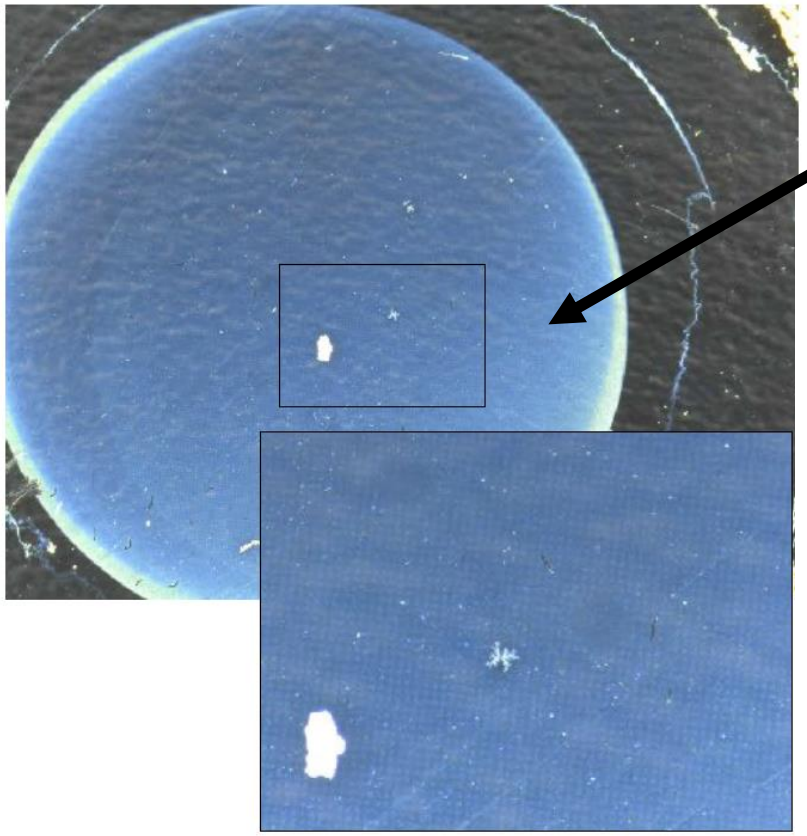

- Ion back flow damages CsI photocathode

Robust photocathodes needed.

Investigating Photocathodes

- For each photocathode material the working point with the best time resolution has to be determined
- The time resolution, quantum efficiency and efficiency are compared
- Reference single photon measurements and tracking data are necessary

And they have to be robust.

Most promissing performance results for non-CsI are from Diamond-Like Carbon (DLC), which also seems robust:

- atmospheric conditions for a few months
- irradiated with pions, in a resistive MM prototye →minimal reduction of Npe/MIP

Different Materials tested like:

- Metallic Photocathodes
- CsI with protection layer
- Nano Diamond Seeding
- Diamond secondairy emitter
- Diamond-like Carbon

3mm MgF + DLC of different thicknesses

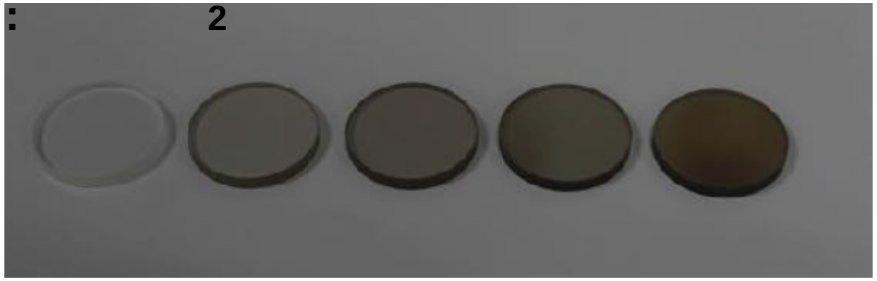

Promising: Diamond Like Carbon (DLC) photocathodes

Diamond-like Carbon

- 2.5 nm DLC time resolution up to 34 ps observed
- Results repeatable in independent samples and Measurements
- Addtitional tests with heating treatment under N2 and H2
- Additional aging tests under pions
- Samples survived rough transport from China

Thickness of DLC film (nm)	Npe/per muon	Detection efficiency for muons
1	Bad	Bad
2.5	3.7	97%
5	3.4	94%
7.5	2.2	70%
10	1.7	68%
5 nm Cr + 18 nm CsI	7.4	100%

PRELIMINARY

2.5 nm DLC in Bulk MM

A/D Voltage	Time Res. (ps)
250/550	37
250/575	34
275/525	38
275/550	34
300/500	39
300/525	34

PRELIMINARY

Towards a large scale detector

Results from a multi-channel prototype

I. Manthos talk

Multi-pad MicroMegas

- Like the MgF /CsI/bulkMM/COMPAS gas single-pad PICOSEC which achieved 24ps per MIP2

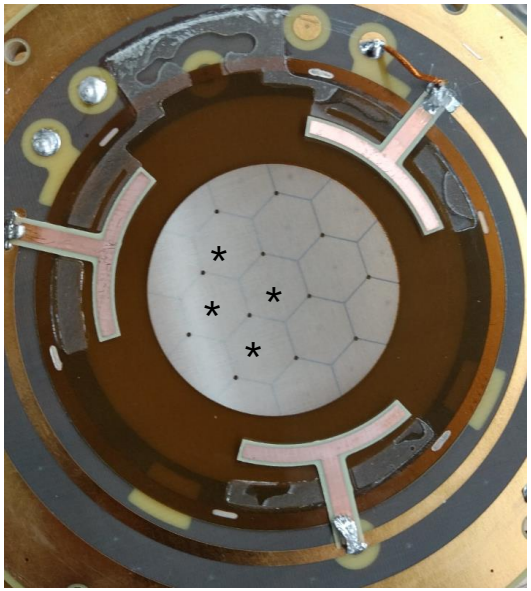

Hexagonal pads 5mm side

Readout 4 pads → 2 osciloscopes

(*** for multi-channel: have to move to chip solutions. Tried SAMPIC, no results yet)

Multi-pad: individual pad response vs. R

- Like the MgF /CsI/bulkMM/COMPAS gas single-pad PICOSEC which achieved 24ps per MIP2

Study response vs. R : distance of track impact from pad center

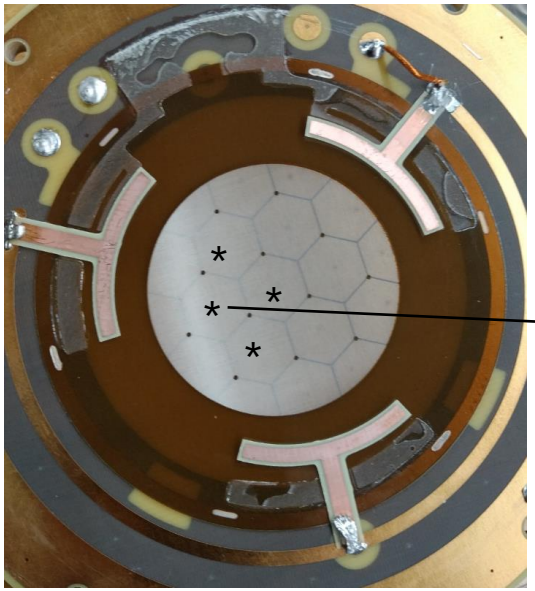

Hexagonal pads 5mm side

0<R<2mm:
full Cherenkov
cone (3mm)
inside pad

4.33 < R < 7.5mm:
Cherenkov cone (3mm)
mostly outside pad

e-peak charge should have all info about where is Cherenkov cone compared to pad. Indeed, universal curves vs. e-peak charge:

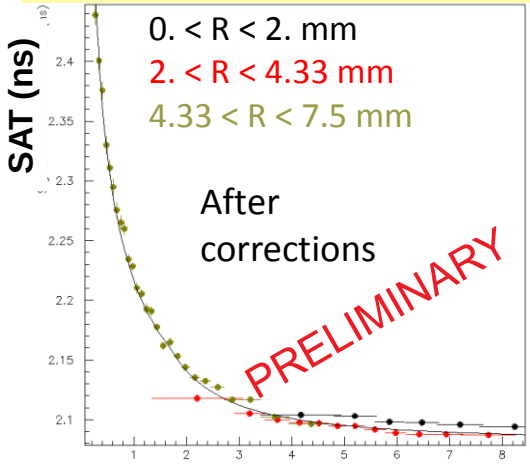

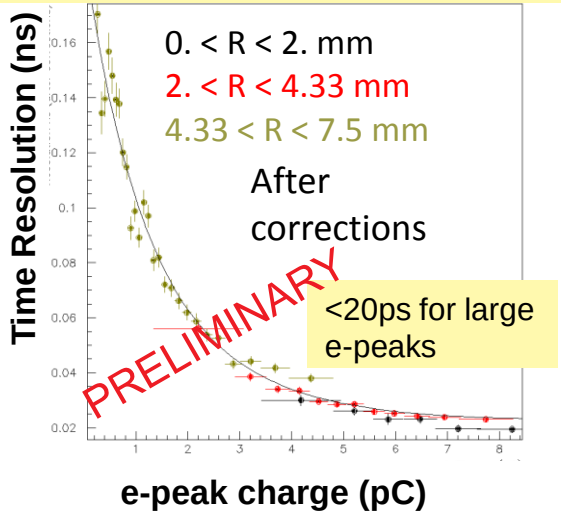

Multi-pad: Same resolution as single-pad

At center of each pad (0<R<2mm):

a time resolution of 25ps for all pads

E.g.:

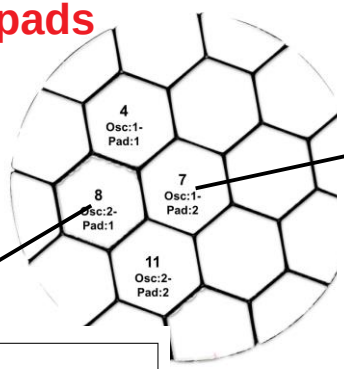

Individual pad response

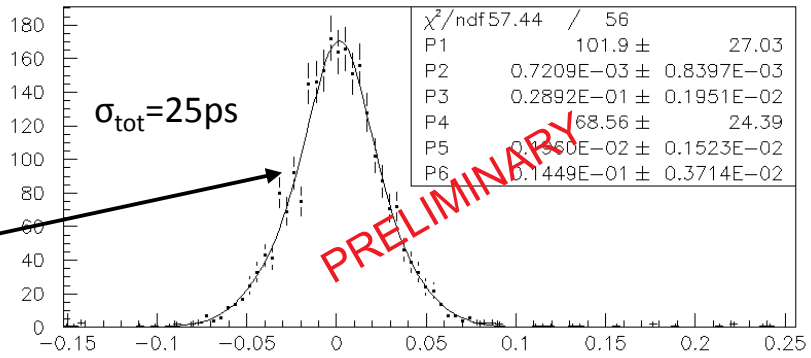

ΔT = Time after all corrections (ns)

Individual pad response

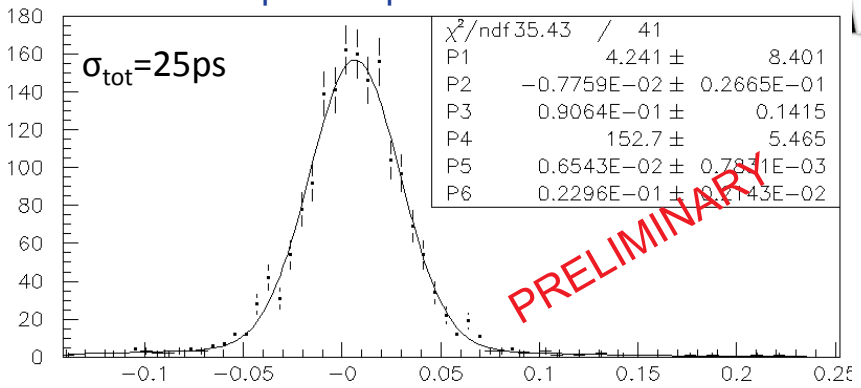

ΔT = Time after all corrections (ns)

Multi-pad: Combining pads

Similar results all across thearea covered by the 4 pads

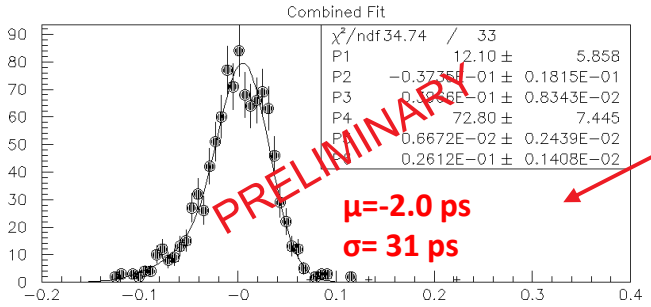

Combining pads event-by-event → Excellent time resolution

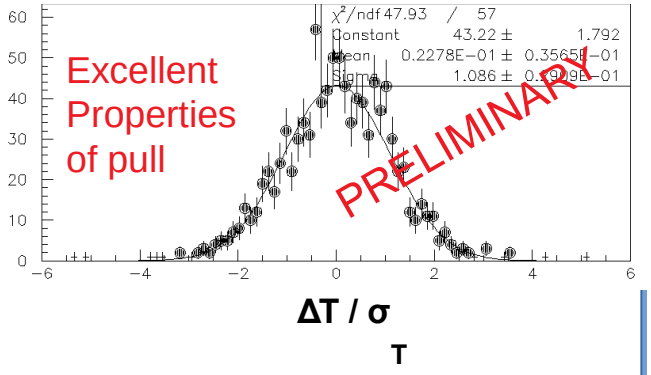

Each individual pad: resolution worsens moving outwards

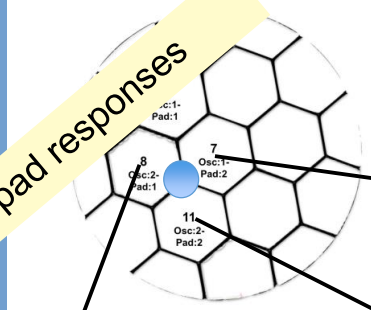

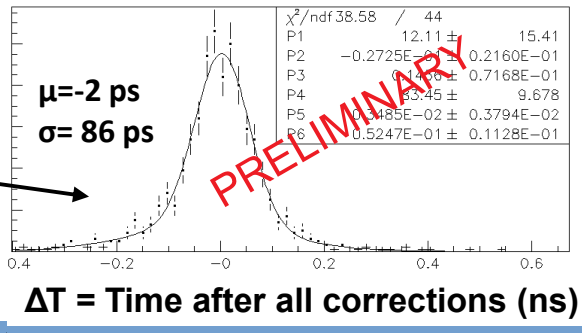

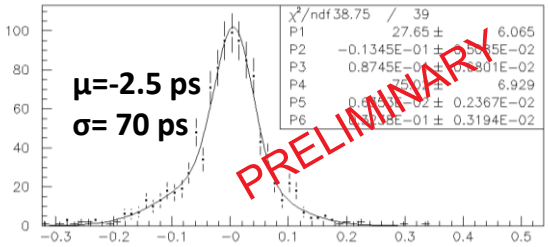

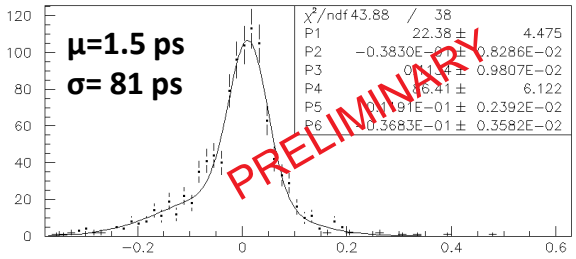

These are not the easiest regions

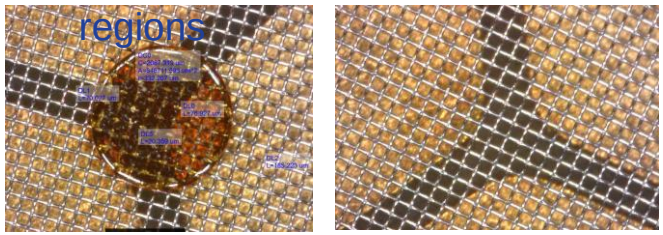

Pilars of ~650μm diameter 200μm inter-pad space

Conclusions

- PICOSEC MicroMegas: a detector with precise timing:
  - Single-channel prototype in Laser and Particle beams
  - 76ps for single photoelectrons, 24ps resolution for timing MIPs
- A well-understood detector:
  - reproduce observed behaviour with detailed simulations and a phenomenological model : valuable tool for parameter-space exploration
- Towards a practical detector: robustness
  - resistive anodes & robust photocathodes: promissing progress
  -
- Towards a large-scale detector: multi-channel
  - response of multi-channel PICOSEC prototype: similar precision as the single-channel prototype, for any impact point of a MIP

RD51 PICOSEC-MicroMegas Collaboration

- **CEA Saclay (France):** D. Desforge, I. Giomataris, T.Gustavsson, C. Guyot, F.J. Iguaz[1], M. Kebbiri, P.Legou, O. Maillard, T. Papaevangelou, M. Pomorski, P. Schwemling, L. Sohl.
- **CERN (Switzerland):** J. Bortfeldt, F.Brunbauer, C. David, J. Frachi, M. Lupberger, H. Müller, E. Oliveri, F.Resnati, L. Ropelewski, T. Schneider, P.Thuiner, M. van Stenis, R. Veenhof[2], S. White[3].
- **USTC (China):** J. Liu, B. Qi, X. Wang, Z. Zhang, Y. Zhou.
- **AUTH (Greece):** K. Kordas, I. Maniatis, I. Manthos, V.Niaouris, K. Paraschou, D. Sampsonidis, S.E. Tzamarias.
- **NCSR (Greece):** G. Fanourakis.
- **NTUA (Greece):** Y.Tsipolitis.
- **LIP (Portugal):** M. Gallinaro.
- **HIP (Finland):** F. García.
- **IGFAE (Spain)**: D. González-Díaz.

1) Now at Synchrotron Soleil, 91192 Gif-sur-Yvette, France
2) Also MEPhI & Uludag University.
3) Also University of Virginia.